Analysis of Large Goss Grains in FeSi Electrical Steels

Dr. Chen, Prof. Raabe

Department for Microstructure Physics, Max-Planck, Düsseldorf

- **Topology**
- **Goss grain evolution during secondary recrystallization**
- **Orientation-dependent dislocation distribution**

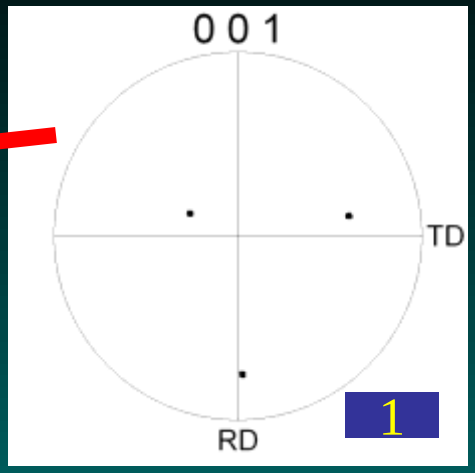

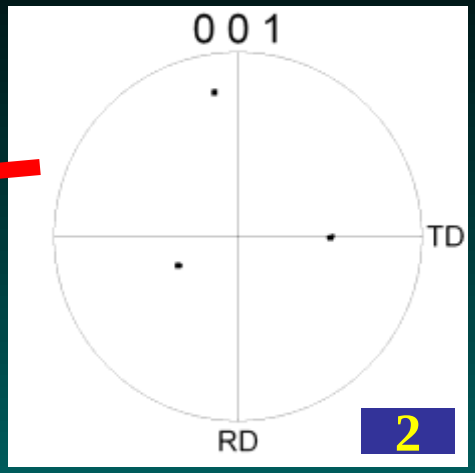

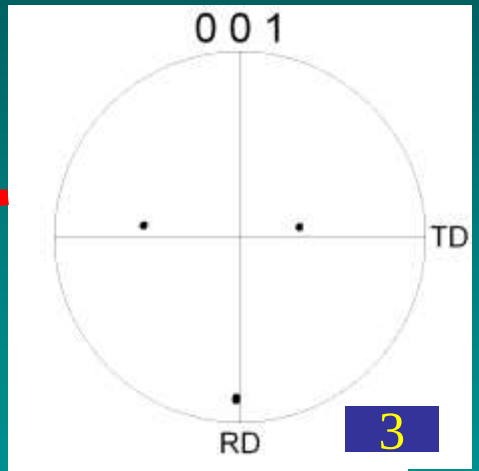

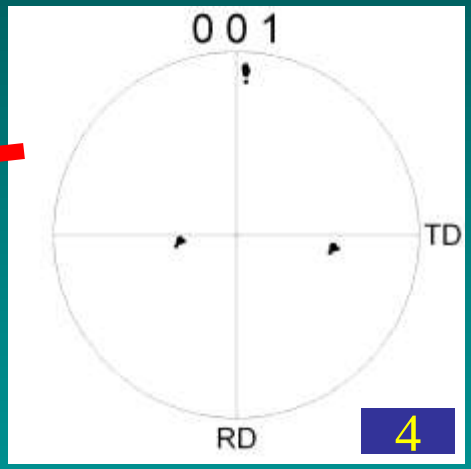

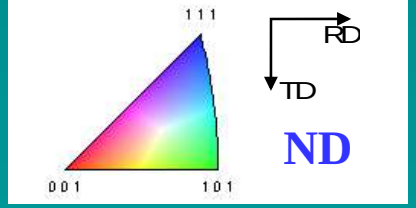

Large grains in recrystallized Si steel

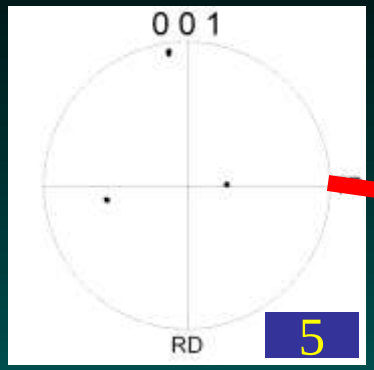

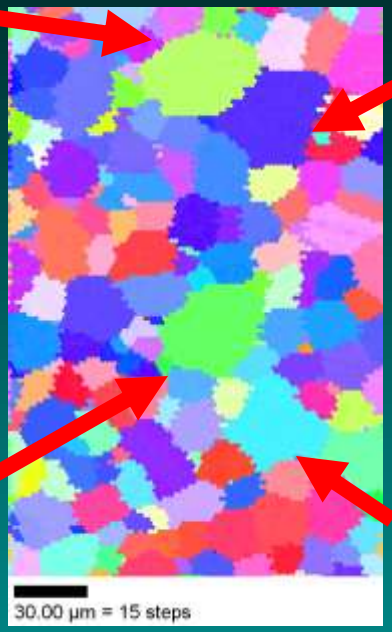

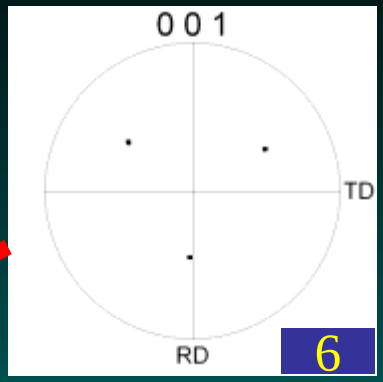

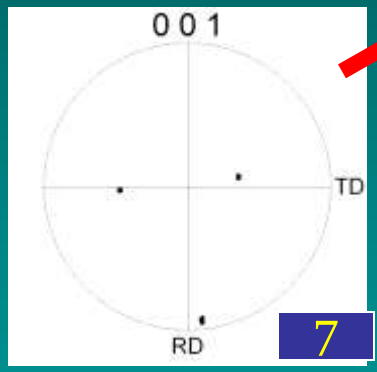

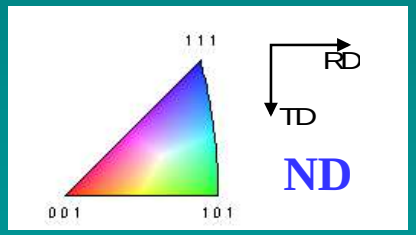

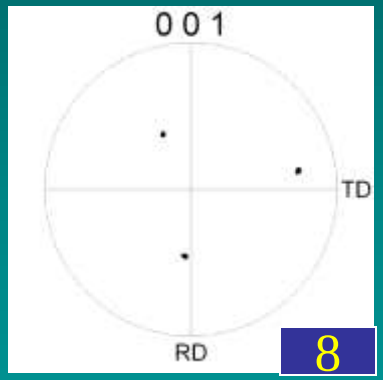

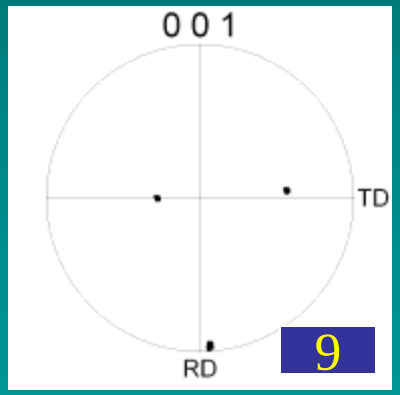

Large grains in recrystallized Si steel

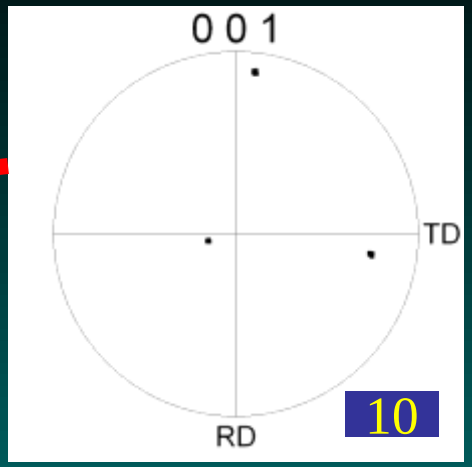

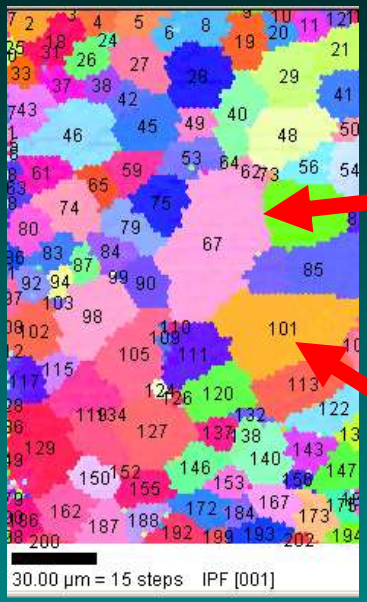

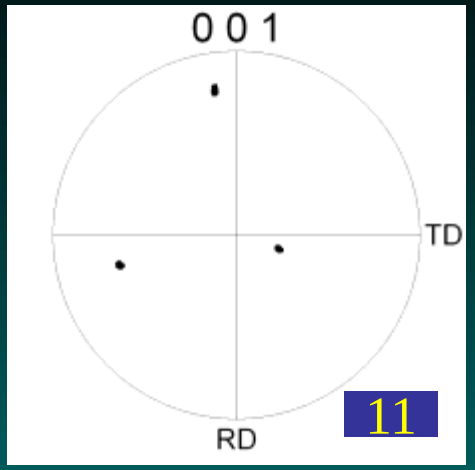

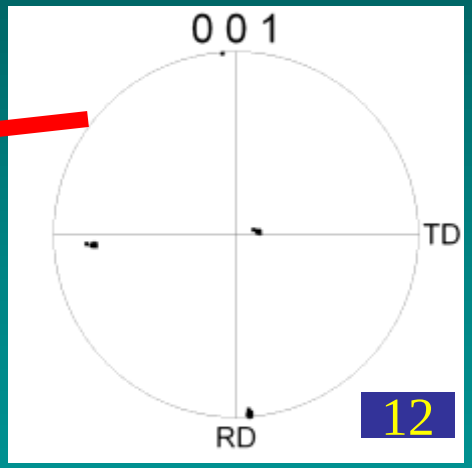

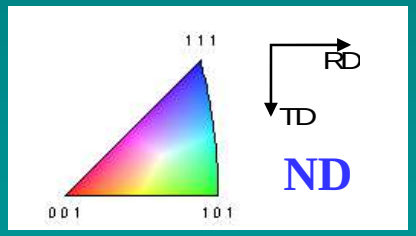

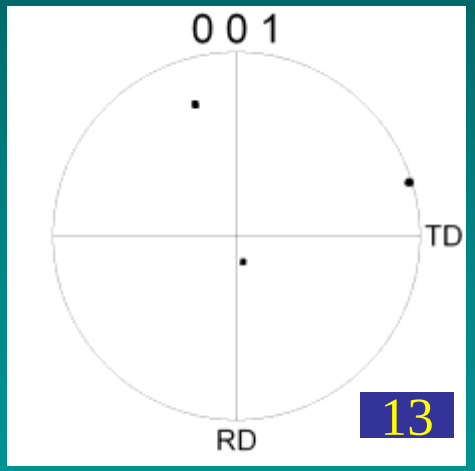

Large grains in recrystallized Si steel

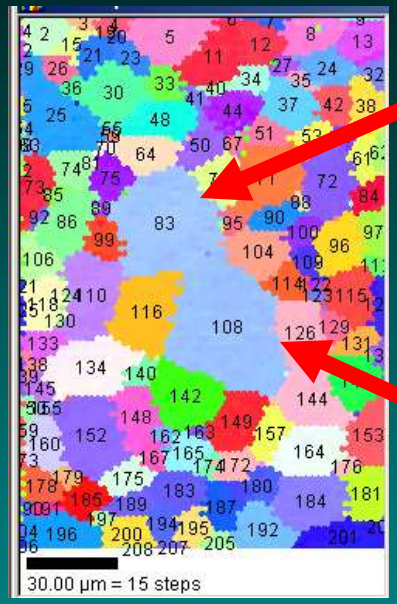

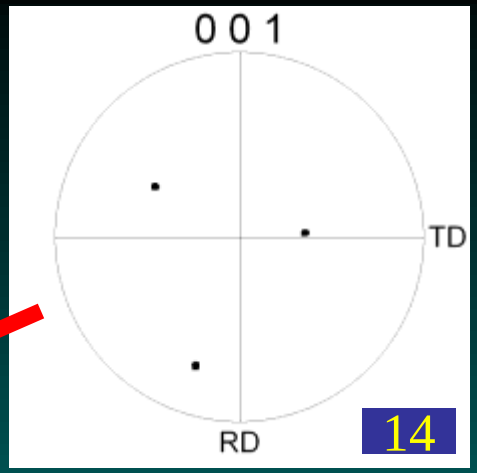

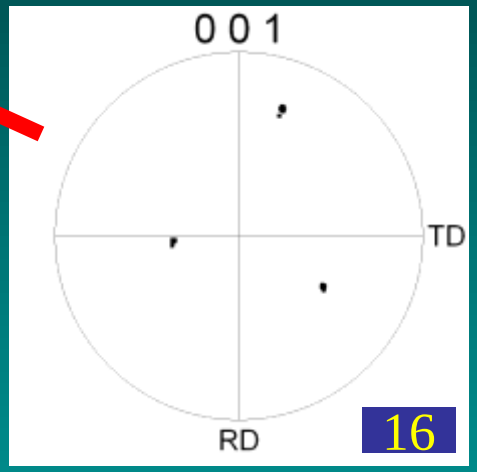

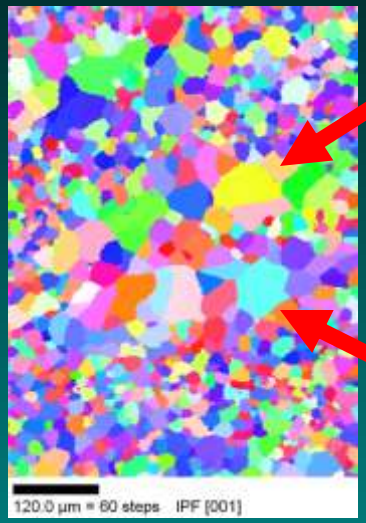

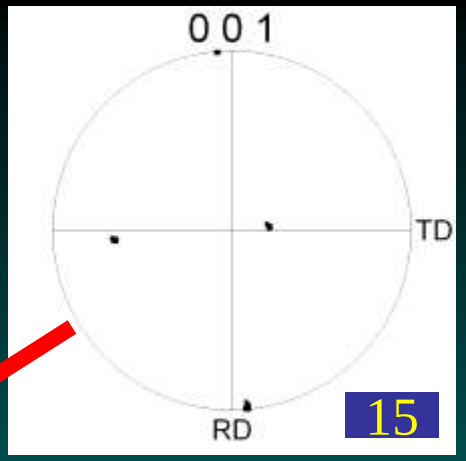

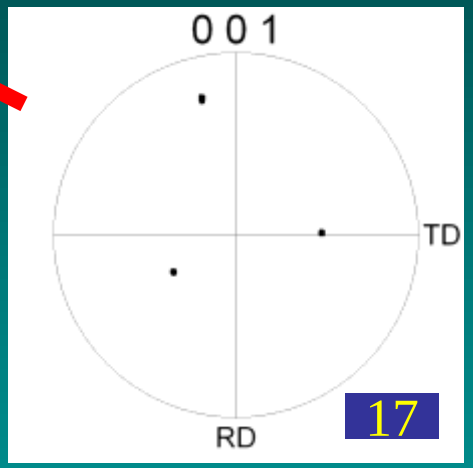

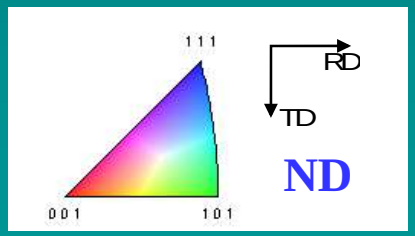

Large grains in recrystallized Si steel

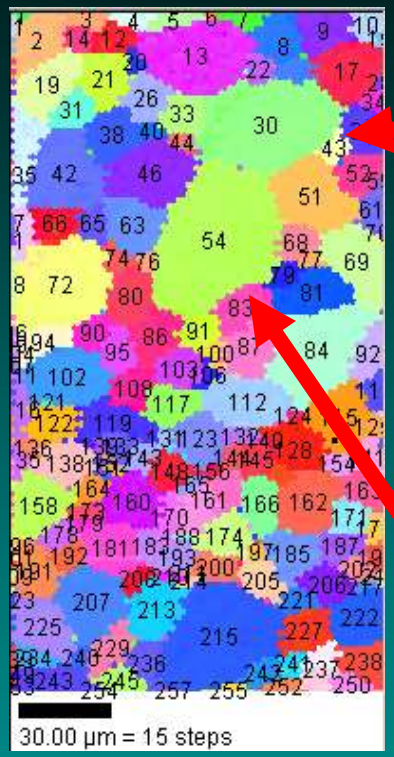

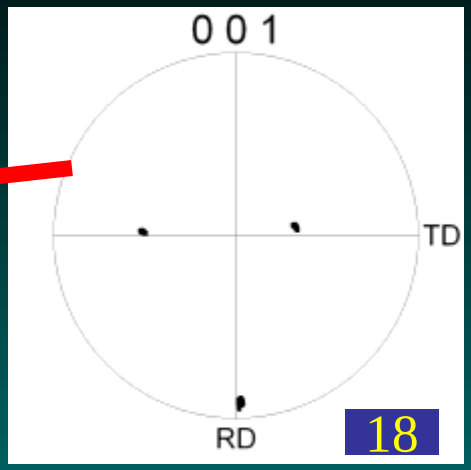

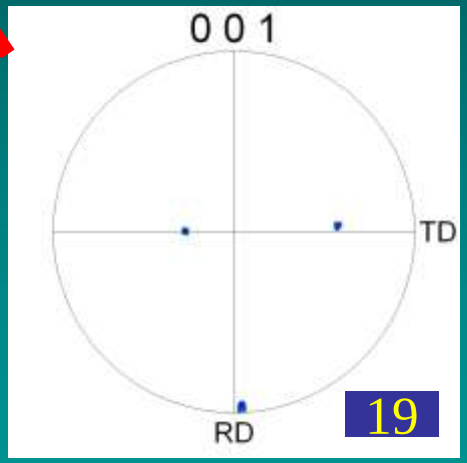

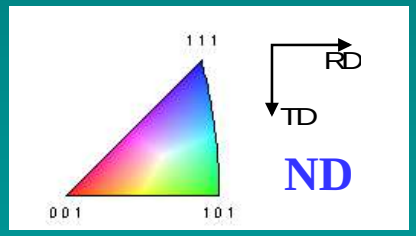

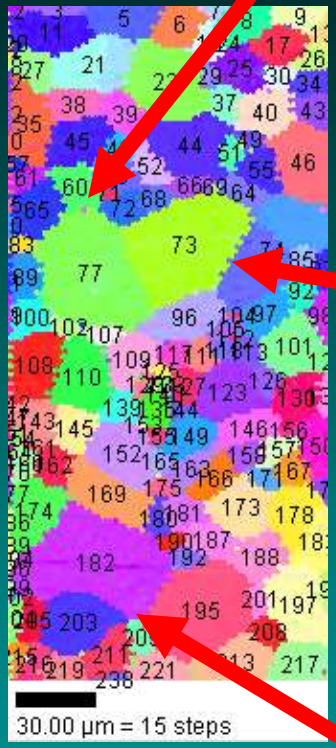

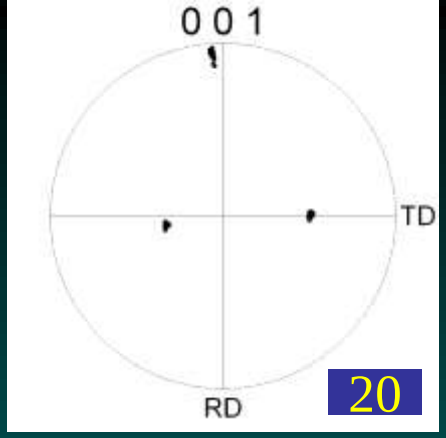

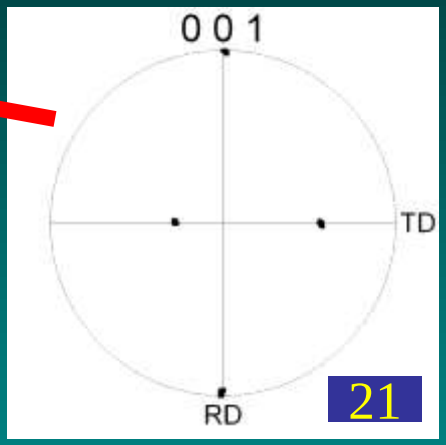

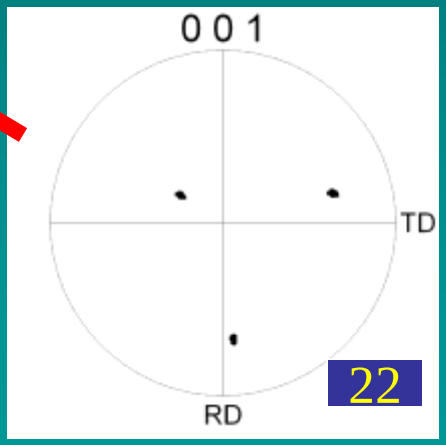

Large grains in recrystallized Si steel

Grain Number	Orientation	Misorientation angle relative to Goss	Area μm^2
1	190.6,62.9,341.3	23.4	2827
2	25.7,39.8,159.2	18.1	2660
3	352.9,55.3,189.6	12.7	2550
4	173.2,56.0,6.5	12.4	1947
5	182.0,31.4,7.0	16.1	1389
6	87.5,48.2,43.5	41.9	1375
7	2.6,50.6,185.0	9.0	1296
8	297.0,45.7,246.3	47.7	1129
9	359.8,31.0,4.7	14.5	1722
10	13.5,17.6,339.0	29.6	1992
11	162.4,27.1,29.2	25.2	1510

Grain Number	Orientation	Misorientation angle relative to Goss	Area μm^2
12	187.4,17.1,177.0	31.4	1739
13	104.3,16.1,273.2	49.3	1178
14	329.4,56.3,20.6	26.1	1050
15	185.8,23.7,178.9	21.9	4365
16	3.9,39.4,331.6	26.2	1410
17	30.5,43.4,338.1	21.4	4562
18	189.4,35.9,170.0	11.6	1102
19	358.1,30.8,5.0	14.7	1552
20	8.3,36.3,354.7	10.4	1445
21	358.3,30.9,0.9	14.3	1399
22	325.9,32.7,43.1	28.8	1632

Average misorientation angle relative to Goss=23.03 degree

Large grains distribution in recrystallized Si steel

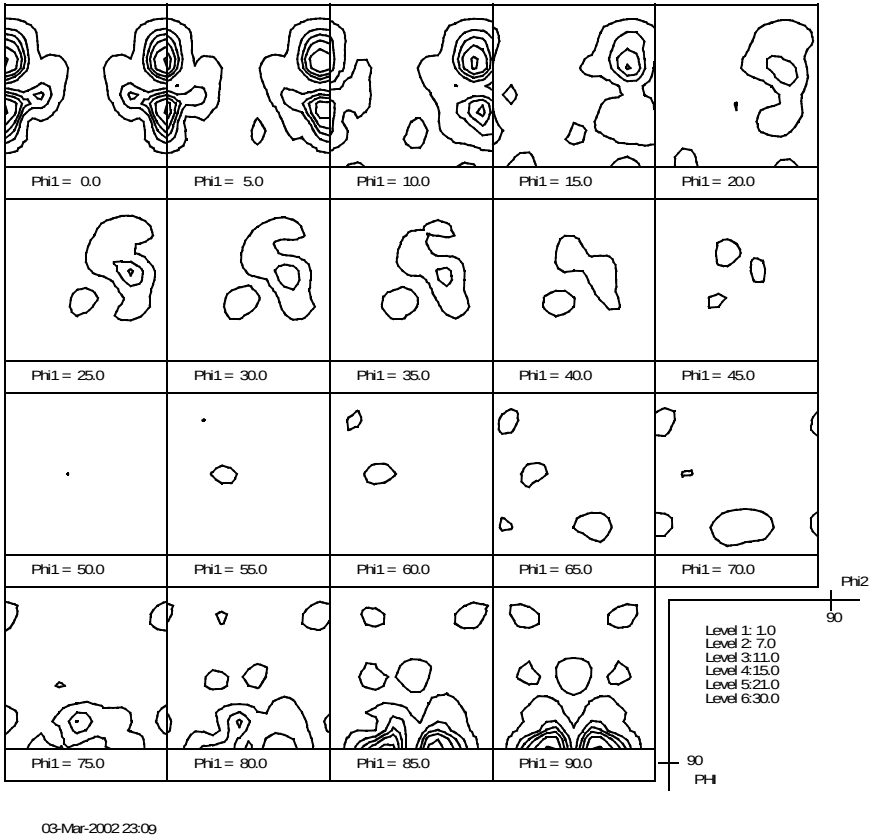

ODF calculated from large grains

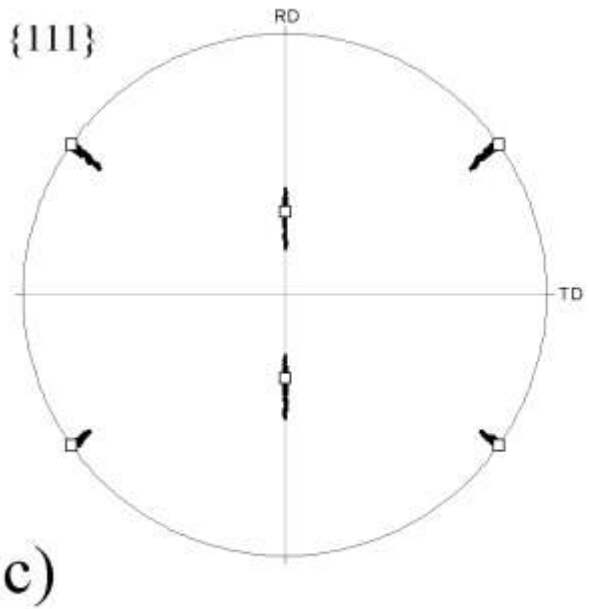

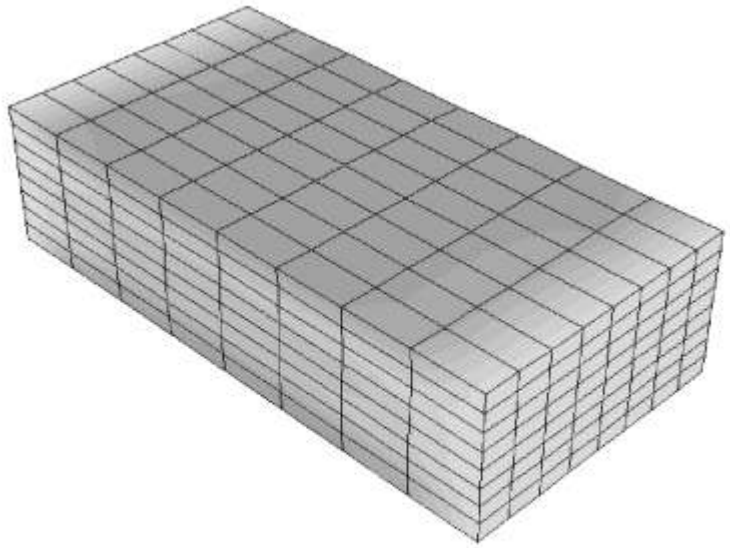

Goss grain splitting during cold rolling

•**All large grains which belong to a large area has been investigated. Average misorientaton angle of these grains relative to Goss grain is about 23 degree. This means that most of these large grains is non-Goss grains.**

•**From the ODF which was calculated from large grains, we can conclude that most of large grains orientation is near to η fiber.**

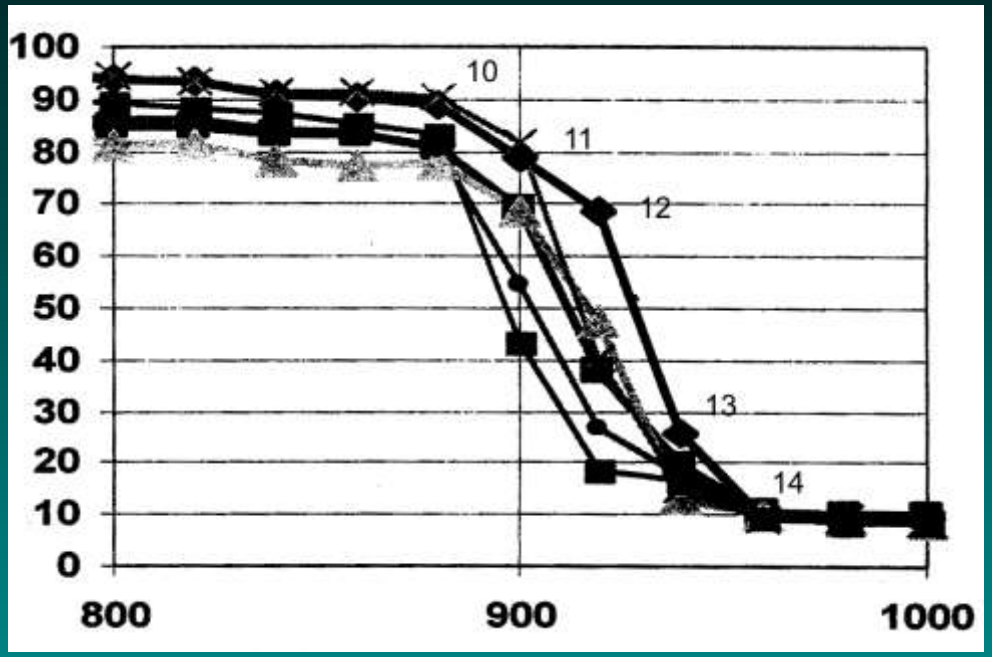

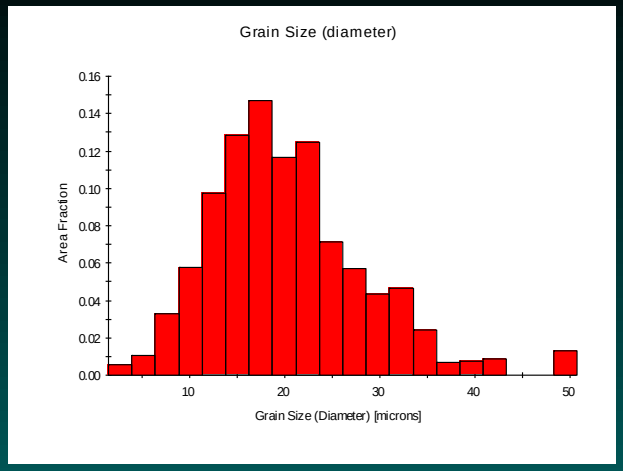

Average grain size of recrystallized sample is 20.3μm

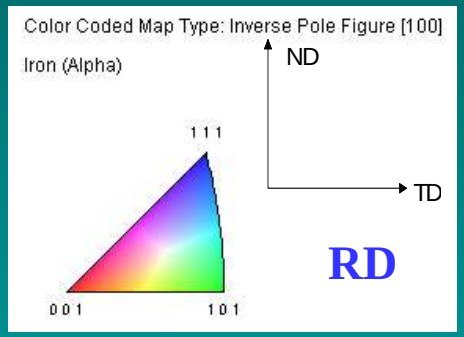

Investigation sample

Average grain size=20.02µm

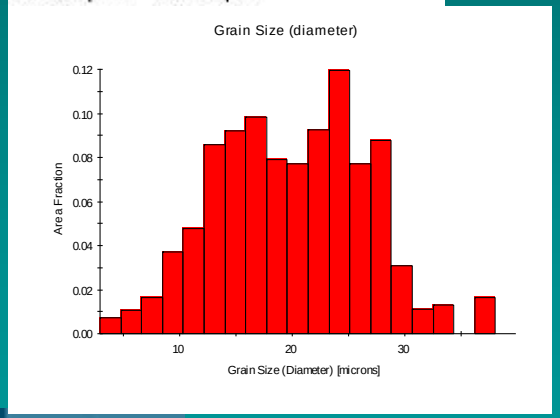

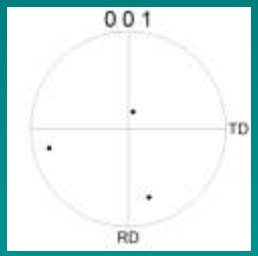

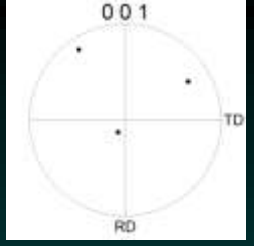

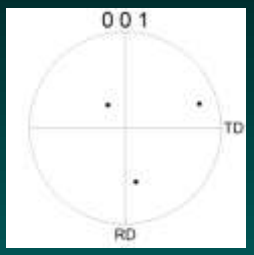

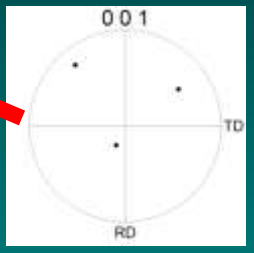

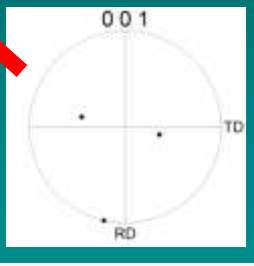

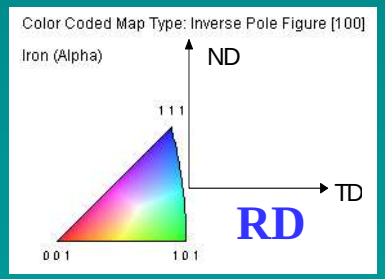

Sample 10.1

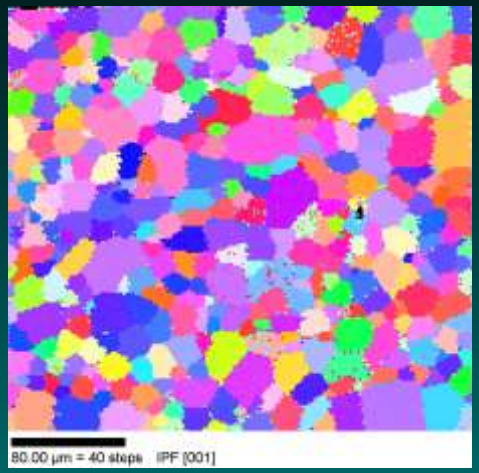

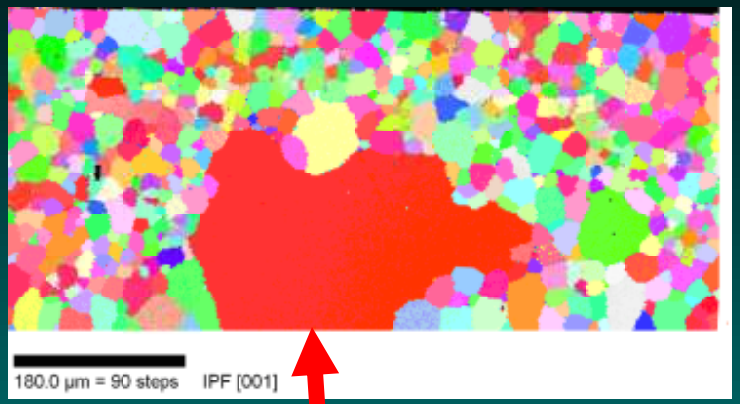

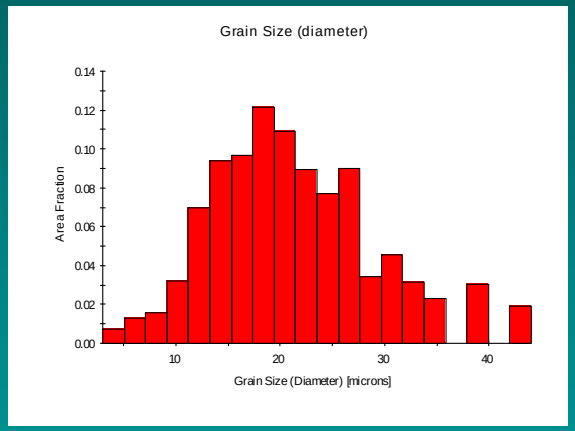

Average grain size=21.32µm

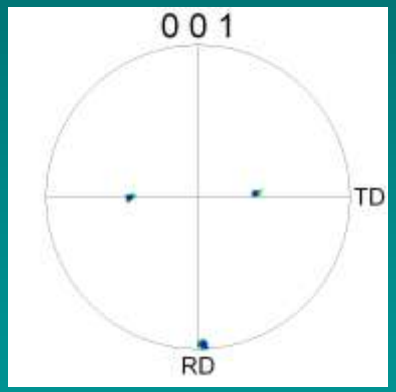

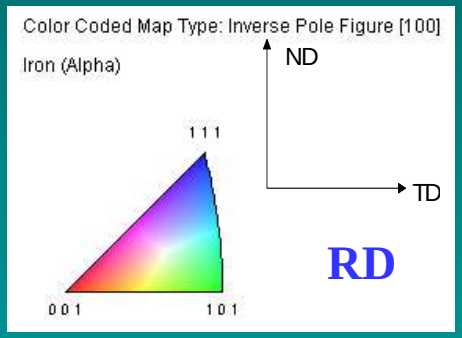

Sample 11.1

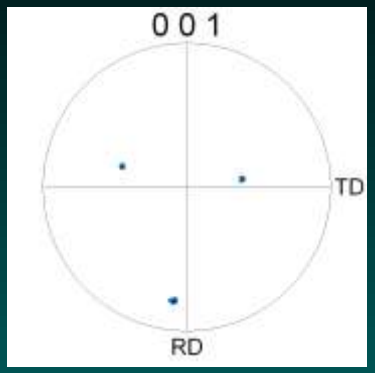

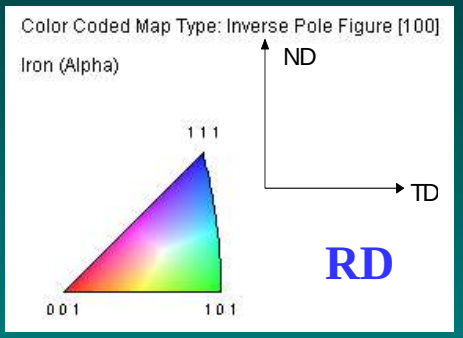

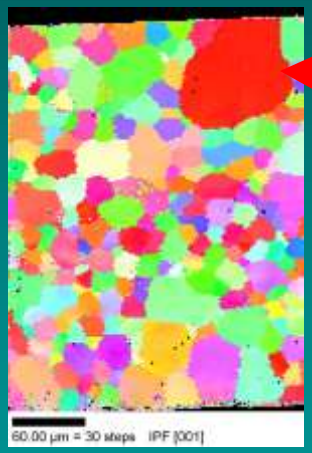

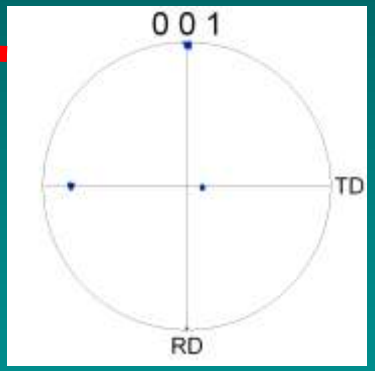

Sample 11.1 (some large non-goss grains)

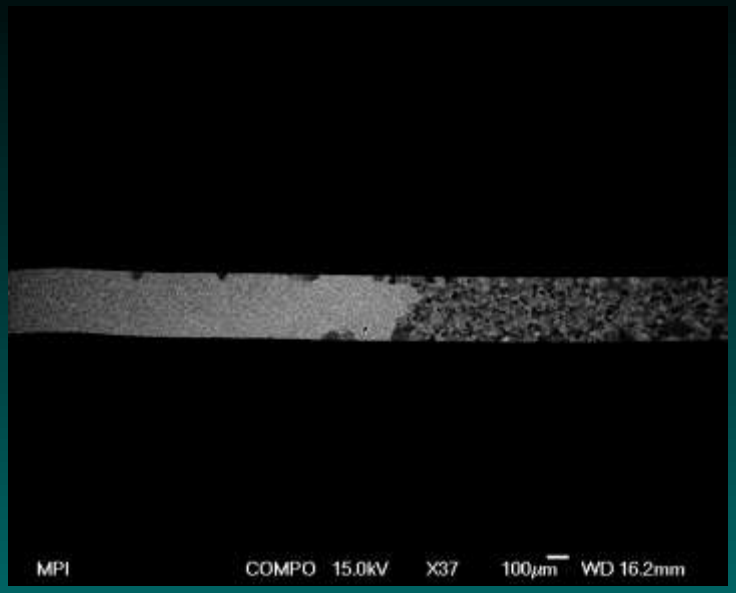
MPI
COMPO 15.0kV X37 100µm WD 16.2mm

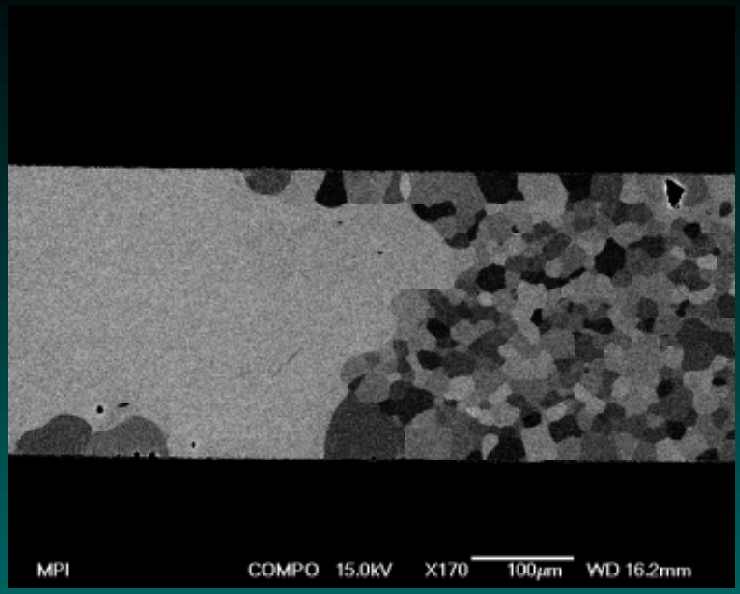
MPI
COMPO 15.0kV X170 100µm WD 16.2mm

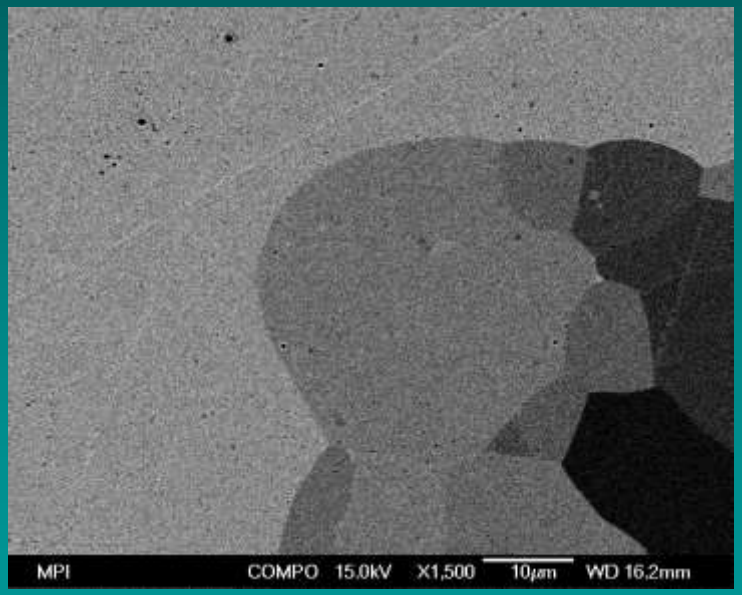
MPI
COMPO 15.0kV X1,500 10µm WD 16.2mm

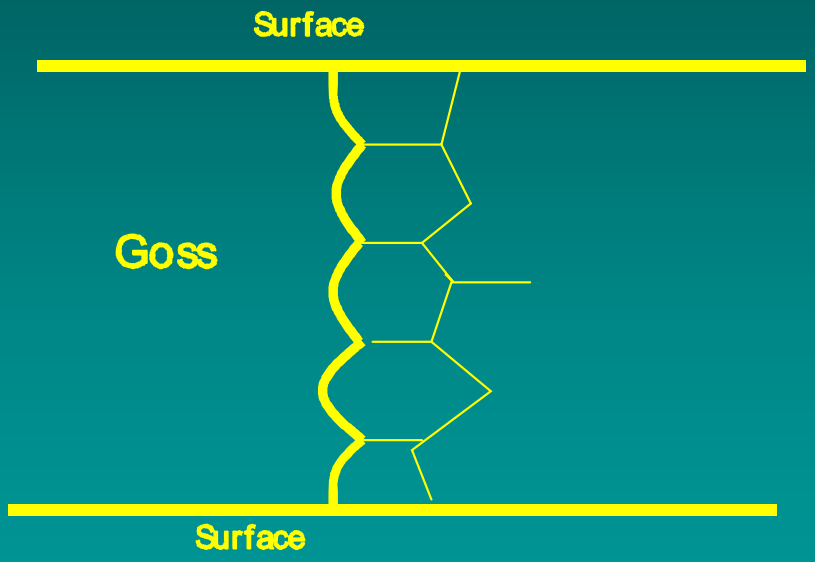
Surface
Goss
Surface

Sample 12.1

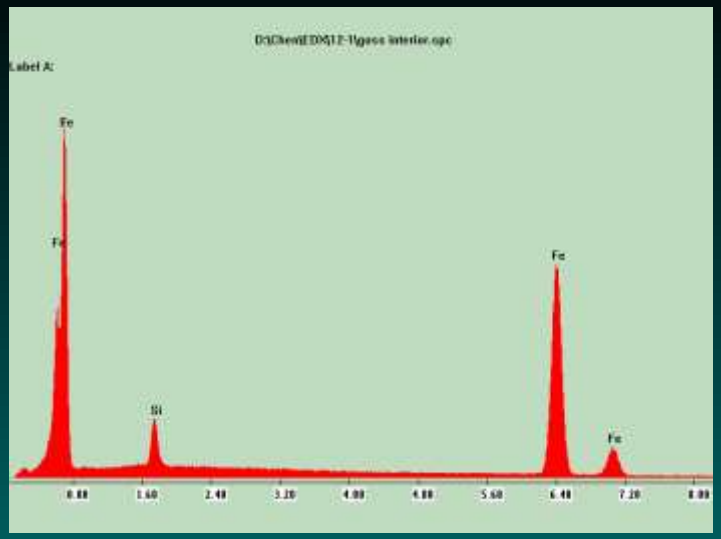

Goss interior

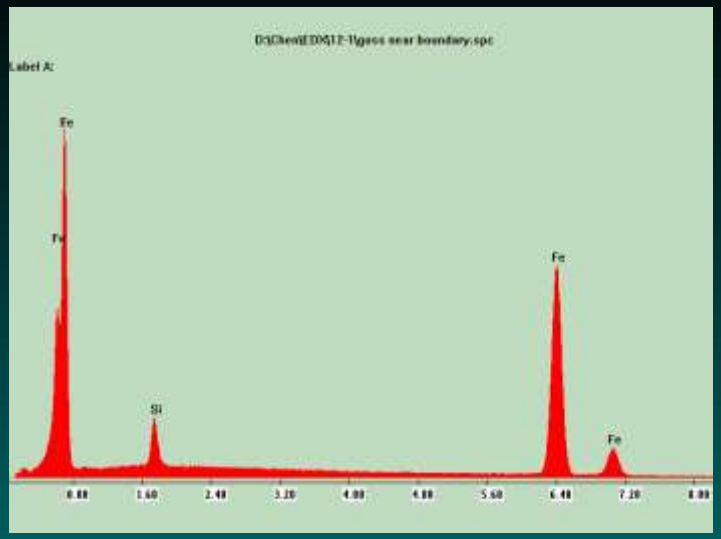

Goss near boundary

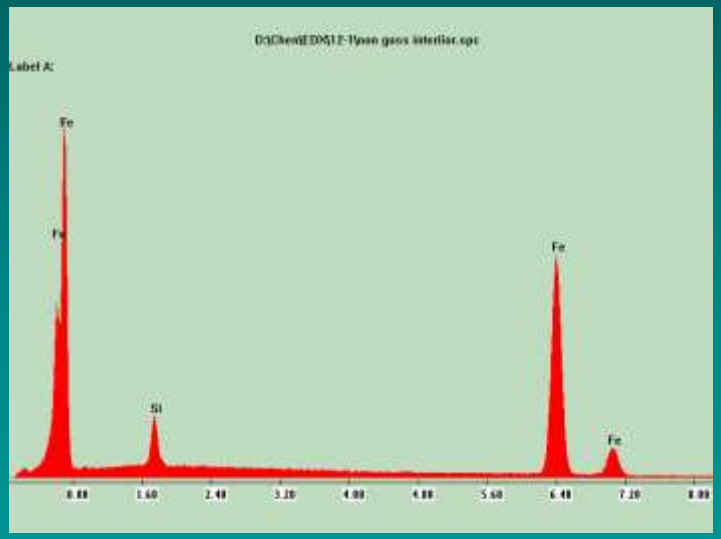

Non Goss grain interior

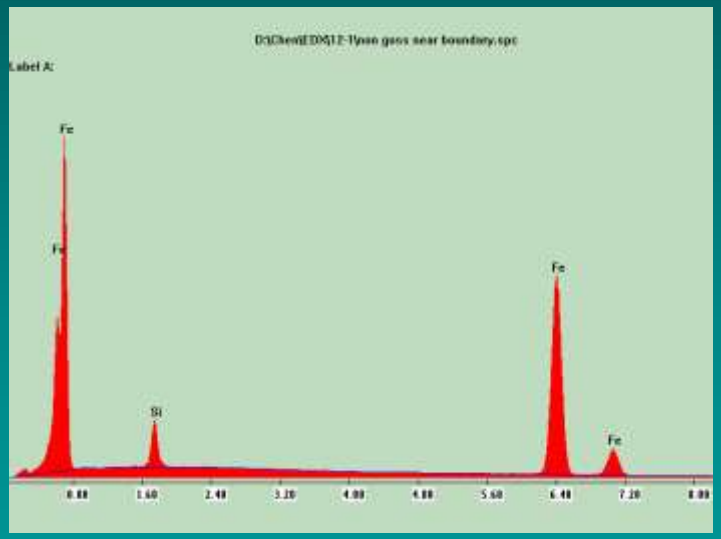

Non Goss near grain boundary

Sample 12.1

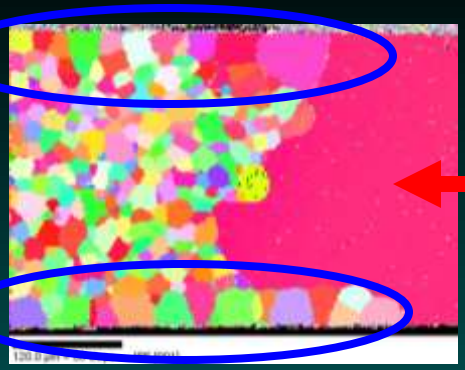

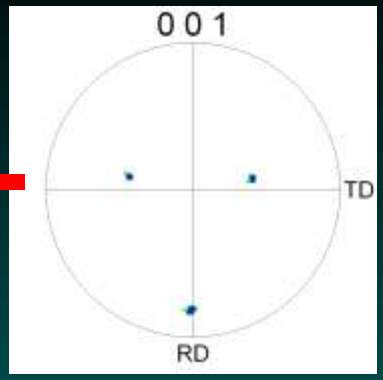

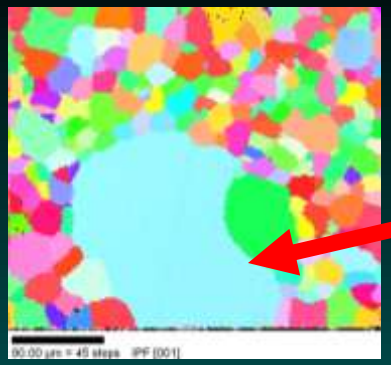

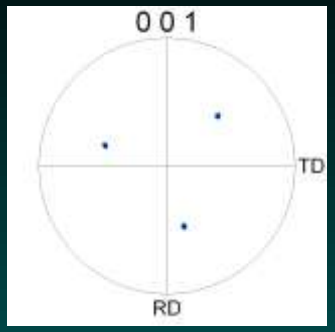

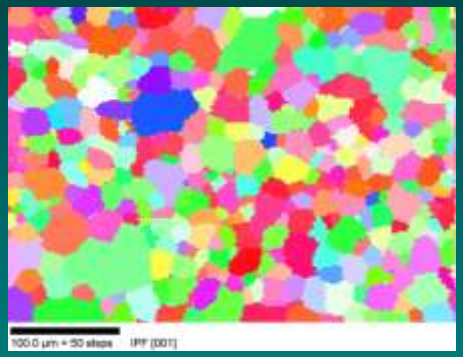

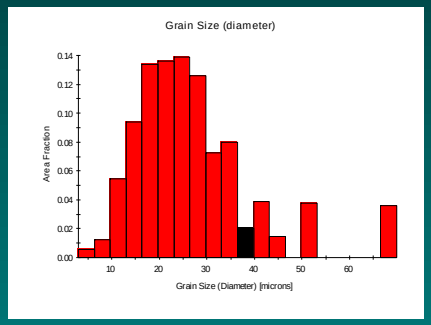

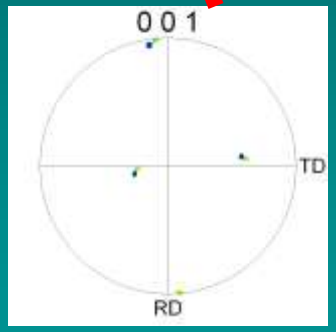

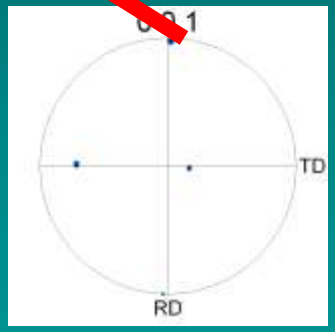

Average non-Goss grains size=26.82µm

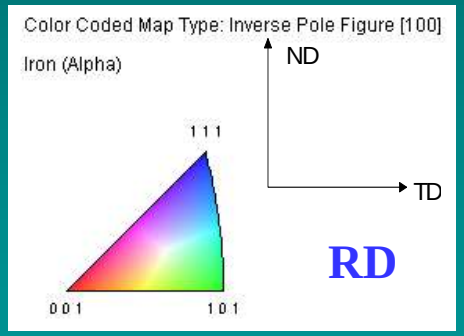

Sample 12.1

Kernal average misorientation

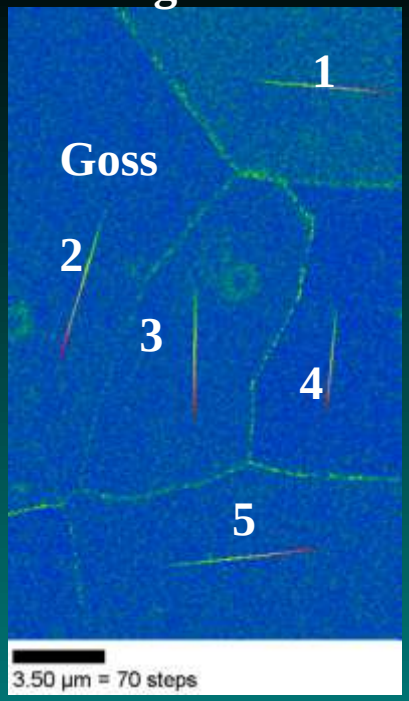

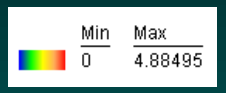

1

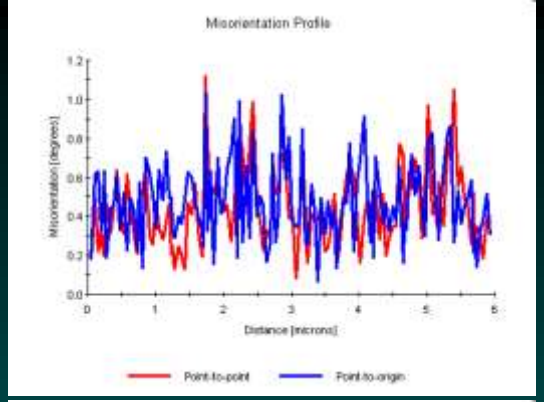

2

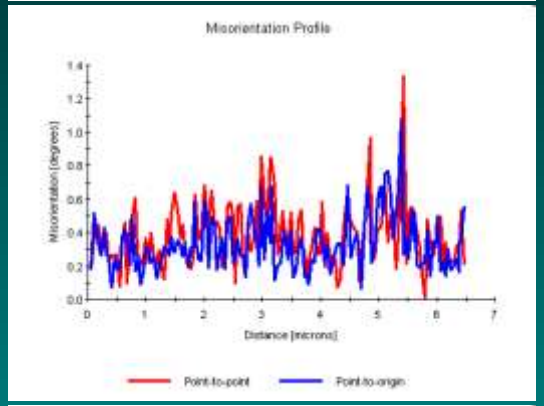

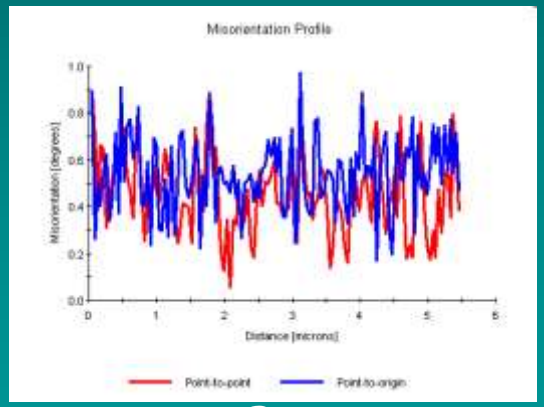

3

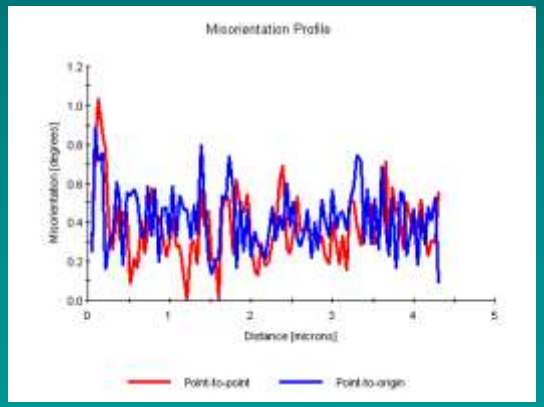

4

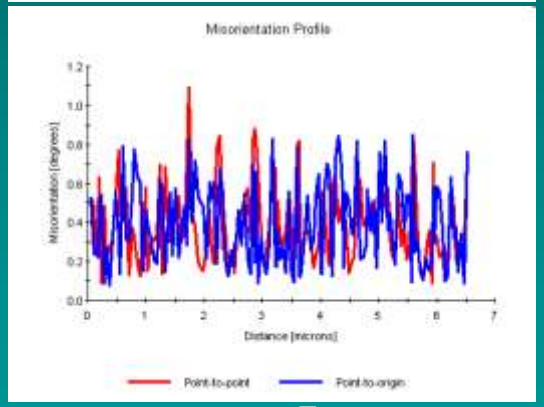

5

Sample 12.1

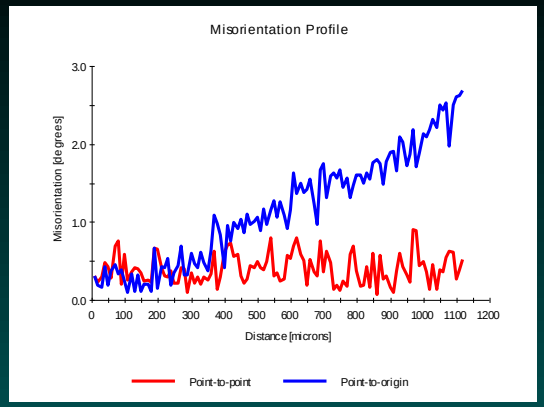

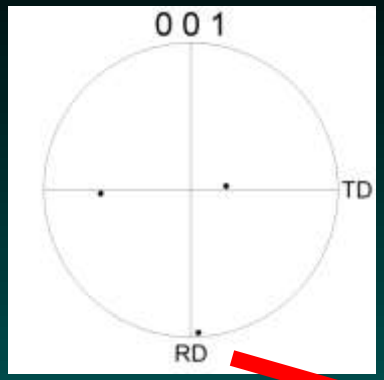

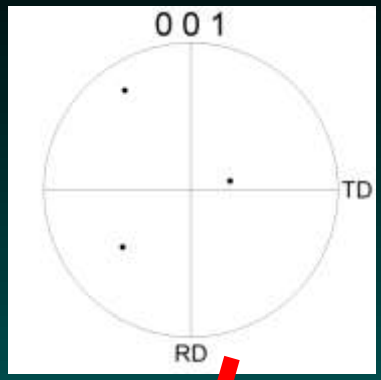

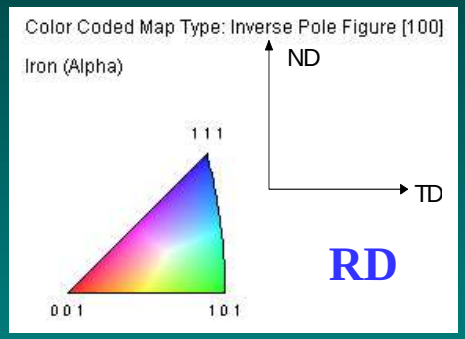

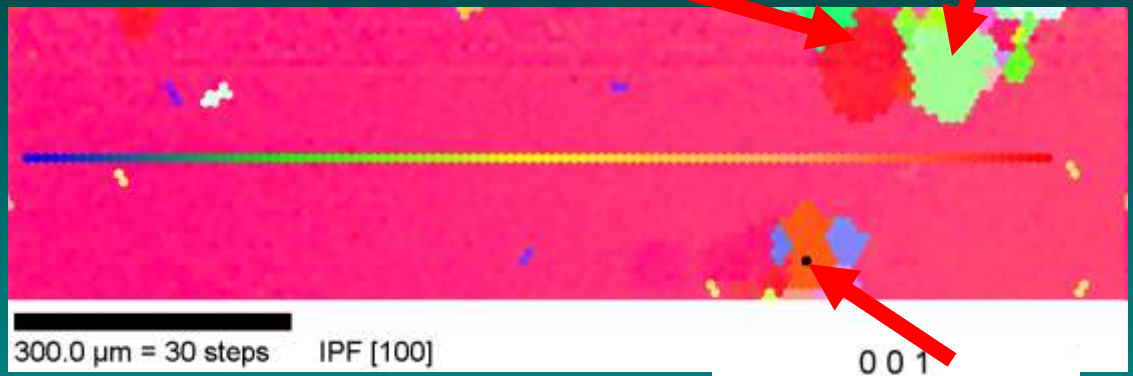

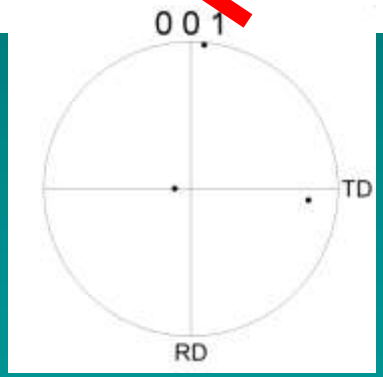

Average orientation gradient=2 degree/mm

Sample 13.1

•There are almost no large Goss grain in sample 10
•In sample 11, there are some large goss grains, but Goss grains doesn't penetrate all sample thickness, Goss grain size is about 100 μm.
•In sample 12, Goss grain penetrate all sample thickness, Goss grain size is about 1 mm and Goss grains grow along the direction within normal plane.
•In sample 13, except few non-goss grains, almost all grains have been eat up by Goss grains.
•In sample 14, secondary recrystallization is finished.
•Chemical composition is almost the same between Goss grain and other grains.
•Orientation gradient is about 2 degree/ mm inside Goss grain.
•In sample 10 and 11, non-goss grain size is the same with that of recrystallized sample. In sample 12, non-goss grain size is a little bit larger than that of recrystallized sample.
•In sample 11 and 12, there are some large non-goss grain, its grain size is from 70-200μm.

Conclusion

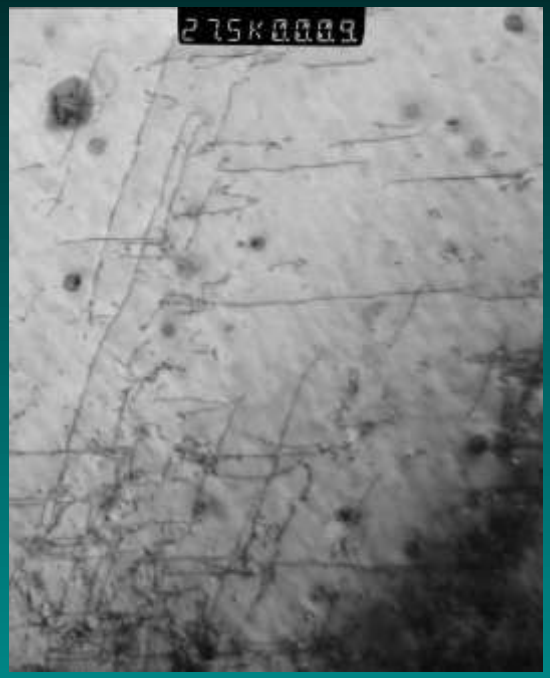

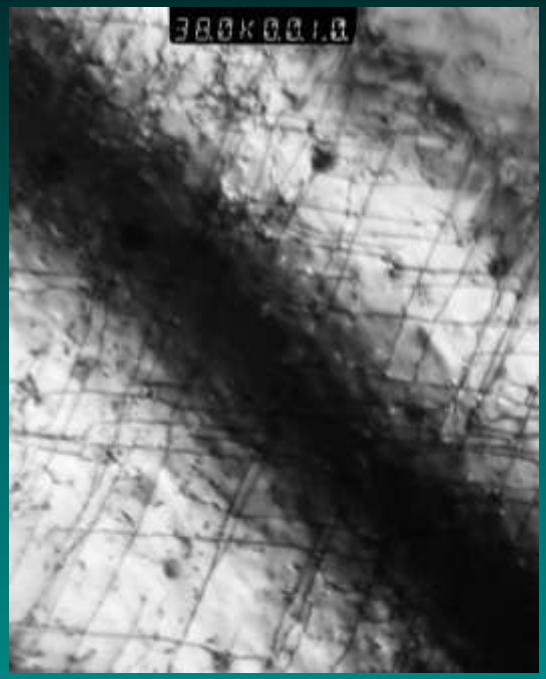

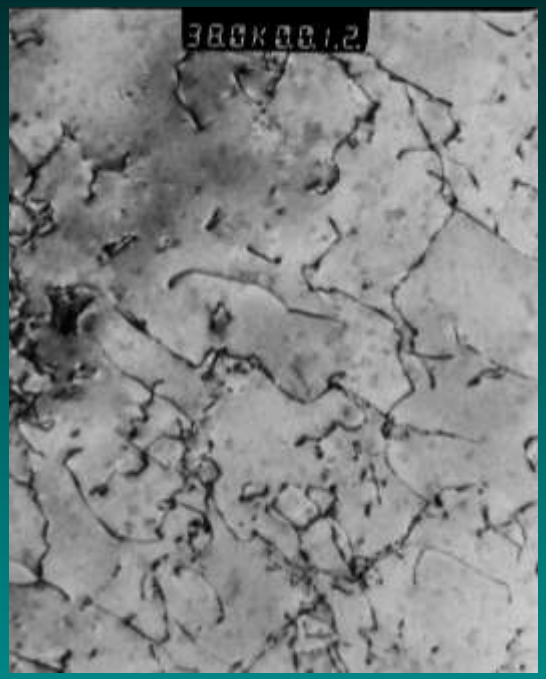

Dislocation in Goss grains

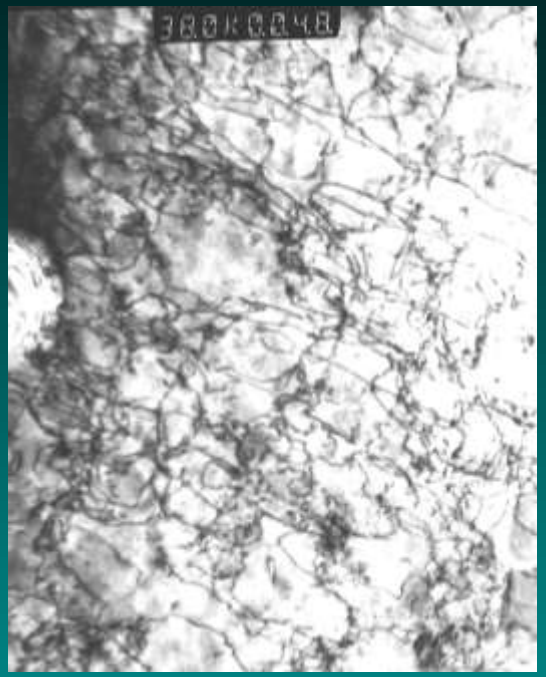

<110>

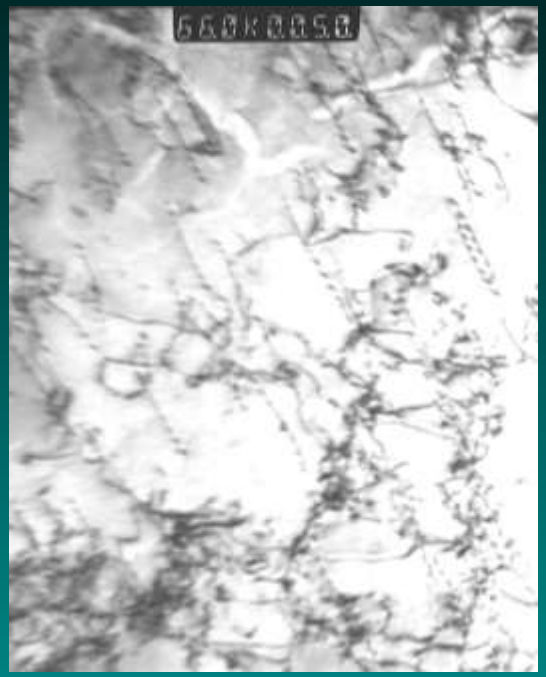

<01-1>

Inhibitor

Dislocation and inhibitor in one Goss grain

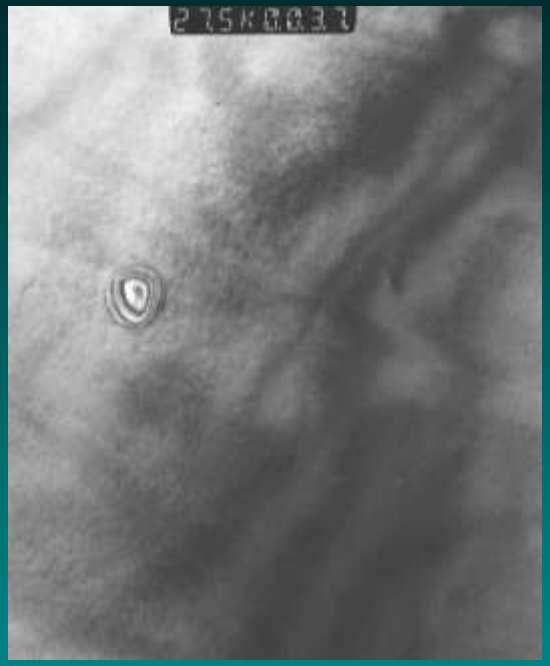

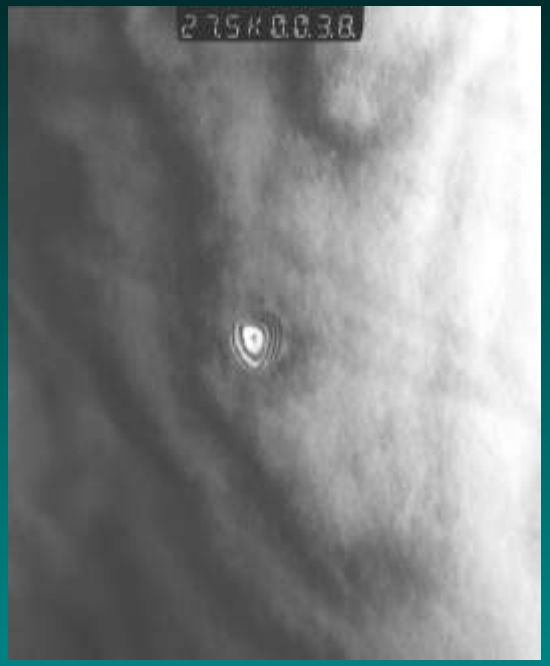

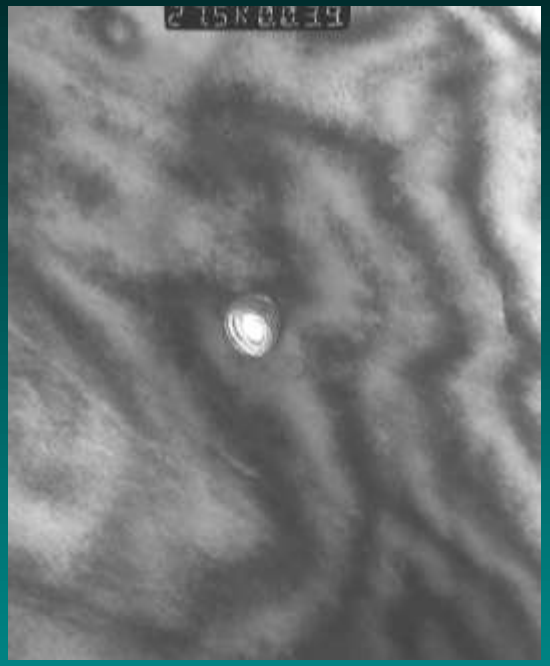

<01-1>

<-1-10>

<101>

One Non-Goss grain)

<011>

<101>

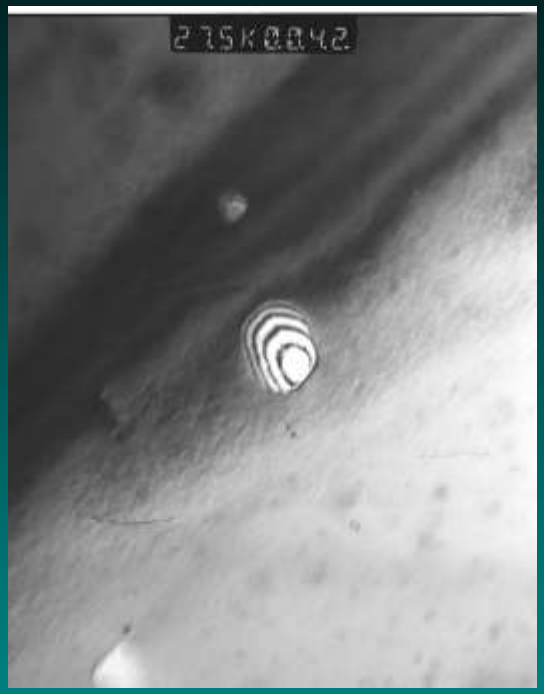

<200>

Dislocation in one non-Goss grain

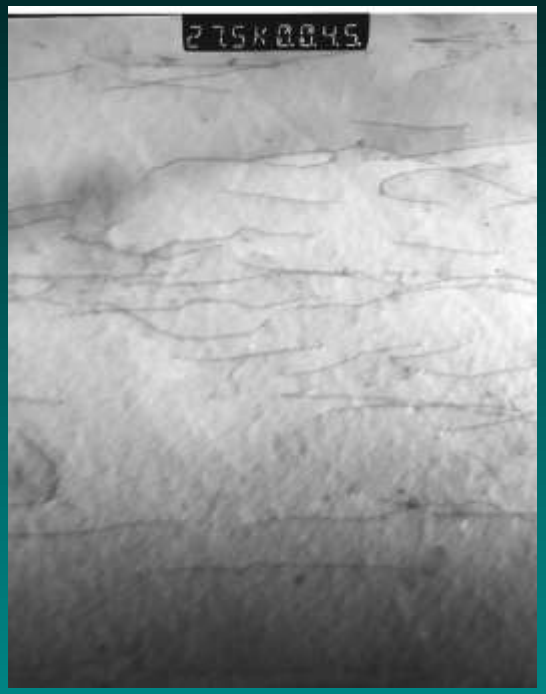

<011>

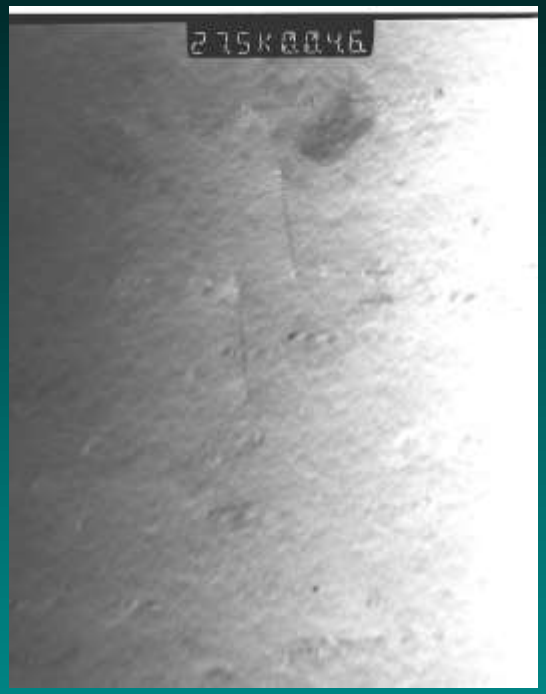

<0-11>

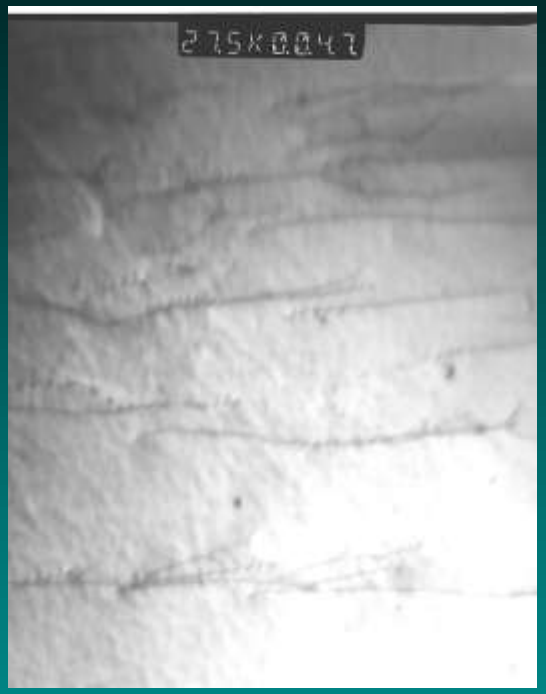

<110>

Dislocation in one non-Goss grain

•There are many dislocations in Goss grains after secondary recrystallization
•After primary recrystallization, dislocation density of grains is very low
•During secondary recrystallization, Goss grains eat up other grains and make a lot of dislocations
•It is possible that these dislocations increase the diffusion coefficient of inhibitor elements, which improves the procedure of particle coarsening.

Materials Science Forum Vols. 495-497 (2005) pp. 1061-1066
online at http://www.scientific.net

Online available since 2005/09/15

Survival of Goss grains during cold rolling of a silicon steel single crystal

Dorothée Dorner[1, a], Ludger Lahn[2] and Stefan Zaefferer[1]

[1]Max-Planck-Institut für Eisenforschung, Max-Planck-Straße 1, 40237 Düsseldorf, Germany

[2]ThyssenKrupp Electrical Steel, Kurt-Schumacher-Straße 95, 45881 Gelsenkirchen, Germany

[a]dorner@mpie.de

Keywords: silicon steel, Goss orientation, cold rolling, single crystal, microband, shear band

Abstract. A silicon steel single crystal with initial Goss orientation, i.e. the {110}<001> orientation, was cold rolled up to 89 % thickness reduction. Most of the crystal volume rotates into the two symmetrical equivalent {111}<112> orientations. However, a weak Goss component is still present after high strain, although the Goss orientation is mechanically instable under plane strain loading. Two types of Goss-oriented crystal volumes are found in the highly deformed material. We suggest that their origin is different. The Goss-oriented regions that are observed within shear bands form during the cold rolling process. In contrast, those Goss-oriented crystal volumes that are found inside of microbands survive the cold rolling.

Introduction

Grain-oriented Fe3%Si steel is a soft magnetic material that is used for iron cores in electrical transformers. It is characterised by a sharp {110}<001> texture, referred to as Goss texture, which develops during secondary recrystallisation in the industrial production process. The origin of the Goss component is in the hot rolling stage, where due to high friction and the resulting shear deformation, the Goss orientation develops close to the sheet surface. The Goss orientation is inherited through the cold rolling and primary recrystallisation process. Finally, during the secondary annealing treatment, some of the Goss grains grow abnormally leading to the sharp Goss texture.

This study aims to investigate the evolution of the microstructure during cold rolling, because in this stage the nucleation sites for the primary recrystallisation of Goss grains are provided. In particular, it is investigated how the Goss-oriented crystal volumes evolve during cold rolling, and how some of the original Goss orientation survives the deformation process although it is known to be instable under plane strain deformation conditions [1-3]. In order to increase the chance to observe Goss grains in the material throughout the deformation process, single crystals of Goss orientation were used as a starting material.

Experimental Method

The experimental procedure of this study comprises growing and subsequent cold rolling of a Goss-oriented single crystal. The starting material for the growth experiment was an industrially hot rolled silicon steel strip containing 3.2 % Si and MnS as inhibitor as used for the production of conventional grain-oriented electrical steel. In the subsequent cold rolling experiment, the single crystal sheet with a thickness of 2.20 mm was cold rolled without lubrication in a laboratory rolling mill with a roll diameter of 105 mm, a roll velocity of 10 m/min, and a load of 120 kN. In 14 passes the sheet was rolled to a thickness of 0.25 mm corresponding to a total engineering thickness reduction of $\varepsilon = 89$ % (true logarithmic strain of $\varphi = 2.2$). The texture and microstructure of the

deformed material was then investigated by automatic crystal orientation mapping based on electron backscatter diffraction (EBSD) in a scanning electron microscope.

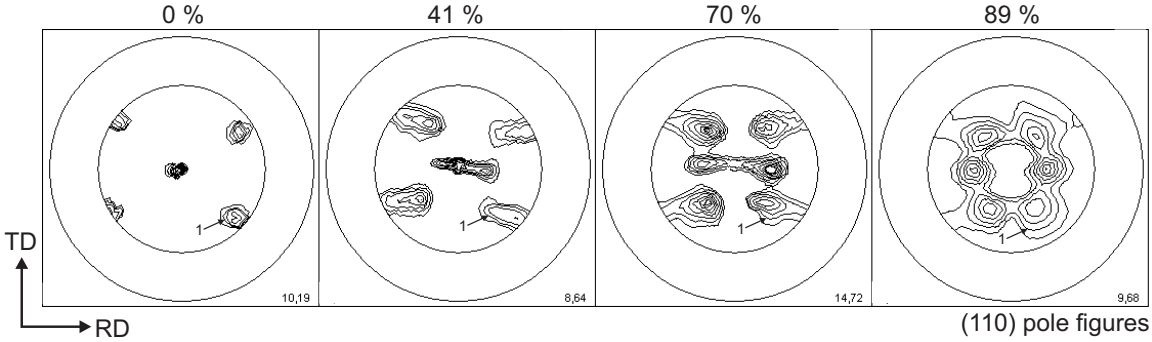

Fig. 1: Texture evolution during cold rolling of an initially Goss-oriented single crystal. (110) pole figures obtained by x-ray diffraction for samples with a thickness reduction of 0 %, 41 %, 70 %, and 89 %, respectively. The {110}<001> orientation rotates 35° around the <110> crystal direction, which is parallel to the transverse sample direction, in both directions into two symmetrically equivalent {111}<112> orientations. TD: transverse direction; RD: rolling direction. The intensity scale for the drawn isolines is logarithmic; the isoline with intensity 1 is indicated by an arrow; the maximum intensity for each sample is given in the lower right corner.

Results

Texture and Microstructure during cold rolling. The bulk texture evolution during cold rolling of the initially Goss-oriented single crystal was investigated using x-ray diffraction. In the course of the deformation process the Goss-oriented single crystal rotates 35° around the <110> crystal direction, which is parallel to the transverse direction (TD) of the sheet, in both directions into two symmetrically equivalent {111}<112> components (Fig. 1). The orientation distribution function for the highest deformed material, as determined by EBSD, is shown in Figure 2 for two sections through the Euler space. The strongest components are the two {111}<112> orientations (Fig. 2a), but the data also show that a weak Goss component is still present after 89 % thickness reduction (Fig. 2b). The evolution of the microstructure was studied in detail using EBSD [4].

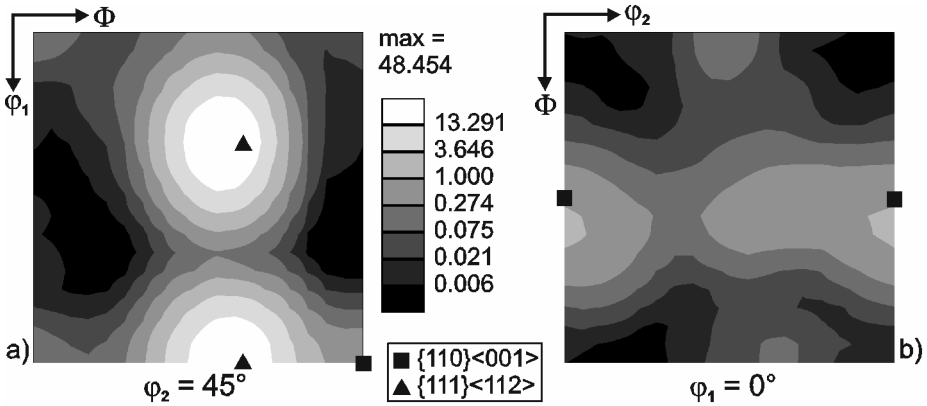

Fig. 2: Texture of the 89 % deformed material. Orientation distribution function diplayed in a $\varphi_2 = 45°$ (a) and a $\varphi_1 = 0°$ section (b) through the Euler space. The texture components with the highest intensities are the two symmetrically equivalent {111}<112> components (a). In addition, a weak Goss component is observed, with a texture intensity of about 1 (b). Note that the texture intensity scale is logarithmic.

Development of Goss-oriented regions during cold rolling. After the highest deformation degree of 89 %, most of the remaining Goss-oriented crystal volume is surrounded by high-angle grain boundaries. After smaller strains of 70 %, some of the Goss-oriented regions are already surrounded by high-angle grain boundaries. Other Goss-oriented regions, however, partly reveal a

continuous orientation gradient to the surrounding {111}<112> matrix and partly form high-angle grain boundaries. The high-angle grain boundaries mostly show an orientation difference of about 35°, which is the misorientation between the Goss and the {111}<112> orientation. These new grain boundaries develop parallel to the transverse direction and are inclined between 10° and 20° to the rolling direction.

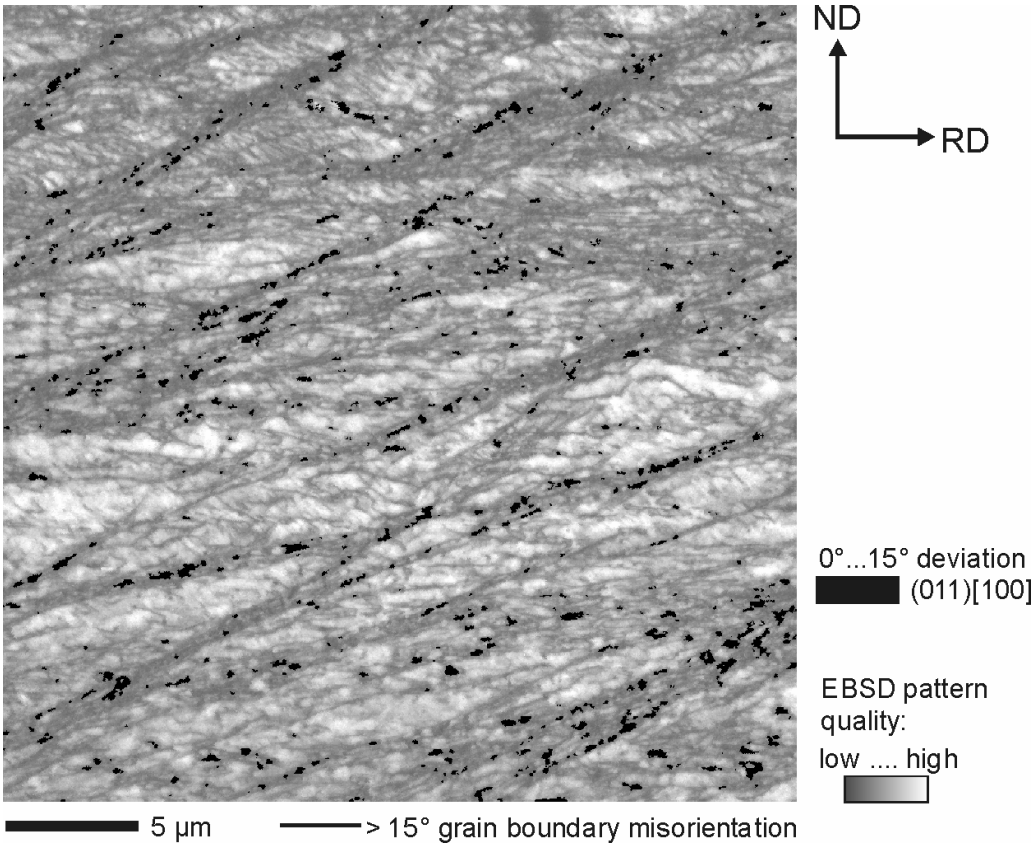

Fig. 3: Goss-oriented regions inside of shear bands in the 89 % deformed material. EBSD pattern quality map (gray scale) showing shear bands as regions with low EBSD pattern qualities. The shear bands are inclined by 29° to 36° to the rolling direction. In addition, Goss-oriented regions are marked in black.

Occurrence of Goss-oriented regions in shear bands and in microbands. Shear bands formed in cold rolled samples with thickness reductions of 77 % and higher [4,5]. When viewed on longitudinal sections, the shear bands are initially inclined by 29° to 36° to the rolling direction, with smaller inclination angles additionally occurring at higher strain [5]. We observed that the inclination direction of the shear bands is dependent on the particular {111}<112> orientation in which they develop [5]. Assuming that the shear band plane is parallel to the transverse sheet direction, we found that it coincides with one {110} plane in both {111}<112> orientations. The texture inside the shear bands consists of the Goss orientation and the two symmetrical {111}<112> components with varying intensities, but no additional orientations appear [5]. These two observations, i.e. the correlation of shear band inclination and crystal orientation and the occurrence of a limited number of texture components inside the shear bands, reveal the crystallographic nature of the observed shear bands. Therefore, we assume that we deal with so-called copper-type shear bands that develop due to geometrical softening as described by Dillamore et al. [6].

We found two types of Goss-oriented crystal volumes in the 89 % deformed material. Most of the Goss-oriented regions are situated inside of shear bands (Fig. 3), which develop at high strain. However, Goss-oriented crystal volumes are also observed inside of microbands (Fig. 4). The observed microbands have a width of about 0.5 µm and their interior is characterised by an EBSD pattern quality that is significantly higher than that within the shear bands.

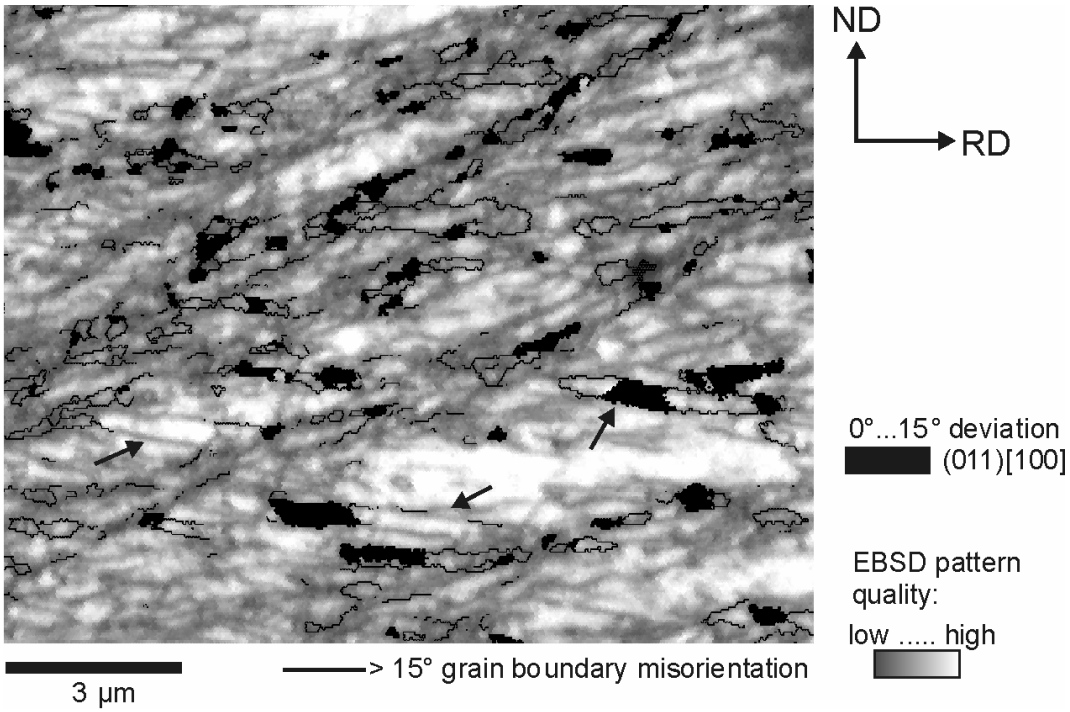

Fig. 4: Goss-oriented regions inside of microbands in the 89 % deformed material. EBSD pattern quality map (gray scale) and Goss-oriented regions (black). Some microbands are marked with arrows. In addition, shear bands are visible.

Discussion

We discuss the stability of the remaining Goss-oriented crystal volumes with respect to two possible types of mechanism [4]: firstly, the development of the Goss orientation in shear bands, and secondly, a microband mechanism that causes some small Goss-oriented crystal volumes not to rotate, although the Goss orientation is mechanically instable under plane strain deformation.

Development of Goss-oriented regions within shear bands. The role of shear bands in the context of the Goss texture formation in silicon steel was already investigated by Haratani et al. [7] and Ushioda and Hutchinson [8]. However, they could not resolve the microstructure of the shear bands in the cold rolled state. In our investigation, we observe that a part of the Goss-oriented regions that are found after high strain is aligned within shear bands (Fig. 3), indicating that this crystal orientation newly forms due to the local shear deformation in the shear bands. We suggest that at first, the initial Goss orientation rotates to the two {111}<112> orientations. Subsequently at higher deformation degrees, when the shear bands are formed, the {111}<112> orientations rotate *back* to the Goss orientation due to the local shear strain state. The alternative possibility that the Goss orientation survives within the shear bands can be excluded because the shear bands first form after most of the Goss-oriented material has disappeared.

Goss-oriented regions between microbands and the development of high-angle grain boundaries. After high strain, Goss-oriented material is not only found inside of shear bands, i.e. in regions with a high dislocation density as indicated by the low EBSD pattern quality, but also in regions inside of microbands, which are characterised by a lower amount of lattice distortion. In this section, a model assumption is outlined explaining the observation of stable Goss-oriented regions inside of microbands as well as the development of high-angle grain boundaries between the {110}<001> orientation and surrounding {111}<112> orientations.

In order to make an estimate about the slip systems that are dominant during the transverse lattice rotation from the {110}<001> into the {111}<112> crystal orientations we used a full constraint Taylor model. For the determination of the Taylor factor, the active slip systems, and the

corresponding shear strain for each slip system, the 12 {110}<111> and the 12 {112}<111> slip systems are taken into consideration. The Taylor-type calculations yield that during the whole deformation and rotation process, one slip system is particularly active (Fig. 5). Moreover, a discontinuous transition of the second and third active slip systems to other active slip systems takes place after a rotation of 10° (Fig 5).

The described microstructural observations combined with the results obtained from the Taylor-type calculation gave reason to propose the following model to explain the survival of the Goss orientation in microbands. During the first deformation stage, microbands develop because slip occurs mainly on one glide system (Fig. 6a). After some deformation, a transition takes place to another set of active slip systems. The microband walls, which developed earlier, now act as a barrier for the motion of the dislocations on the newly active slip systems causing the dislocations to pile up at the microband walls (Fig. 6b). At locations where the width of the microbands is small, further dislocation activity is impeded inside the microbands due to these pile-ups (Fig. 6c). Therefore, no further lattice rotation takes place within the microbands. By this process, the Goss orientation might survive within small crystal volumes and high-angle grain boundaries develop around the Goss orientation when the lattice rotation continues in the region next to the microband. The presented model assumption explains the survival of the initial Goss orientation in small crystal volumes due to a *microband mechanism*, i.e. no back rotation of the crystal lattice is involved in this process. This is in contrast to the origin of the Goss-oriented regions inside the shear bands.

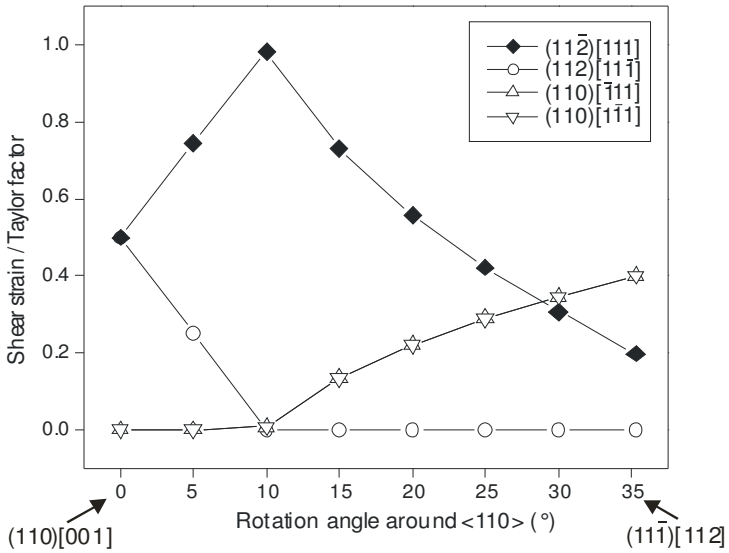

Fig. 5: Shear strain normalized by the Taylor factor as a function of rotation from (110)[001] to (11-1)[112] around the <110> crystal direction. The shear strain is concentrated on only one slip system. After 10° rotation the second and third active slip system changes. The Taylor-type calculations were performed with 24 slip systems for a bcc crystal.

Summary and Conclusions

A silicon steel single crystal with {110}<001> crystal orientation was cold rolled and the evolution of the Goss orientation during rolling deformation was investigated using EBSD.

(1) The texture after cold rolling up to 89 % thickness reduction is characterised by two strong symmetrically equivalent {111}<112> components. In addition, a weak {110}<001> component is still present though the Goss orientation is mechanically instable under plane strain loading.

(2) In the highly deformed material, most remaining Goss-oriented regions are situated inside of *shear bands*. However, Goss-oriented crystal volumes are also found inside of *microbands*. We suggest that their origin is different. One type of Goss-oriented regions newly form at higher deformation degrees due to shear deformation within the shear bands. The Goss-oriented regions that are found outside of the shear bands are suggested to survive during plane strain deformation in small regions within microbands. We propose that the microband walls act as barriers for dislocation glide on other glide systems. Due to dislocation pile-ups further rotation of Goss-oriented volumes is impeded and the Goss orientation survives.

3) The sharp Goss orientation that develops during secondary recrystallisation in industrially processed silicon steel has its origin in the hot rolling process. In this study, we observed two types of Goss-oriented regions after cold rolling of an initially Goss-oriented single crystal. Provided that our results on single crystals can be transferred to polycrystalline material, it might be concluded that the Goss-oriented regions that are found in microbands and that are assumed to be stable during cold rolling, have special significance for the formation of Goss grains in the primary recrystallised material, and, consequently, for the abnormal growth of Goss grains during secondary recrystallisation. If the newly formed Goss-oriented regions within the shear bands were specifically relevant, then the removal of the surface layer would not change the formation of Goss grains during primary recrystallisation as it was described in literature [9-11].

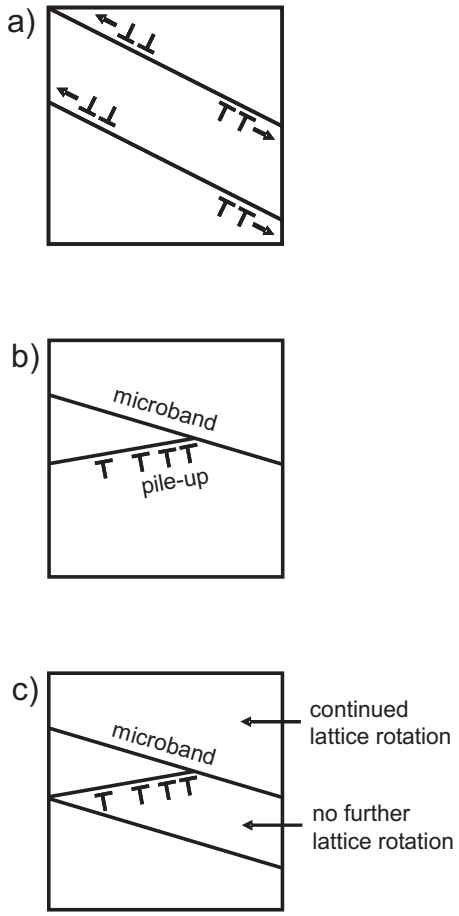

Fig. 6: Scheme of the model explaining the survival of Goss-oriented crystal volumes in regions inside of microbands.

Acknowledgements

The authors gratefully acknowledge financial support by ThyssenKrupp Electrical Steel. The same company also kindly provided the sample material for this research project. We thank Mrs. B. Schaff for growing the single crystals.

References

[1] M. Hölscher, D. Raabe and K. Lücke: Steel Research Vol. 62 (1991), pp. 567-575

[2] M. Hölscher, D. Raabe and K. Lücke: Acta Metallurgica et Materialia Vol. 42 (1994), pp. 879-886

[3] D. Raabe, Z. Zhao, S.-J. Park and F. Roters: Acta Materialia Vol. 50 (2002), pp. 421-440

[4] D. Dorner, S. Zaefferer and D. Raabe: Acta Materialia, submitted

[5] D. Dorner and S. Zaefferer: Proceedings of the 2nd International Conference on Texture and Anisotropy of Polycrystals, Metz, France, submitted

[6] I.L. Dillamore, J.G. Roberts and A.C. Bush: Metal Science Vol. 13 (1979), pp. 73-77

[7] T. Haratani, W.B. Hutchinson, I.L. Dillamore and P. Bate: Metal Science Vol. 18 (1984), pp. 57-65

[8] K. Ushioda and W.B. Hutchinson: ISIJ International Vol. 29 (1989), pp. 862-867

[9] A. Böttcher and K. Lücke: Acta Metallurgica et Materialia Vol. 41 (1993), pp. 2503-2514

[10] S. Mishra, C. Dährmann and K. Lücke: Acta Metallurgica Vol. 32 (1984), pp. 2185-2201

[11] N.C. Pease, D.W. Jones, M.H.L.Wise and W.B. Hutchinson: Metal Science Vol. 15 (1981), pp. 203-209

Available online at www.sciencedirect.com
SCIENCE DIRECT
Journal of Magnetism and Magnetic Materials 304 (2006) 183–186
Journal of magnetism and magnetic materials
www.elsevier.com/locate/jmmm

Overview of Microstructure and Microtexture Development in Grain-oriented Silicon Steel

Dorothée Dorner[a], Stefan Zaefferer[a,*], Ludger Lahn[b], Dierk Raabe[a]

[a]*Max-Planck-Institut für Eisenforschung, Max-Planck-Strasse 1, 40237 Düsseldorf, Germany*
[b]*ThyssenKrupp Electrical Steel GmbH, Kurt-Schumacher-Strasse 95, 45881 Gelsenkirchen, Germany*

Available online 13 March 2006

Abstract

This paper outlines the development of the microstructure and microtexture of grain-oriented silicon steel during the industrial production process. In particular the evolution of the Goss orientation was studied in industrial material as well as in single crystal experiments.

PACS: 61.14.−x; 75.50.Bb; 81.40.Ef; 92.10.Ns

Keywords: Grain-oriented silicon steel; Goss orientation; EBSD

1. Introduction

The grain-oriented silicon steel is a soft magnetic material that is used as the core material in electrical transformers. It is characterized by a pronounced Goss texture, i.e. a $\{110\}\langle 0\,0\,1\rangle$ preferred crystal orientation. This sharp texture develops due to a discontinuous or abnormal Goss grain growth during a high-temperature annealing at the end of the industrial production process. Although it is a matter of intensive basic and applied research since more than 50 years, there is no general agreement on the origin of preferred growth of the Goss grains. It is known, however, that the inheritance of Goss orientation from early production stages plays an important role, as it was shown by Böttcher and Lücke in Ref. [1] who removed the Goss-containing surface layer of the hot rolled material with the result that abnormal Goss grain growth did not take place after further processing. Therefore, in this contribution we intend to outline the evolution of the Goss orientation in industrially processed grain-oriented silicon steel along the various production stages, i.e. hot rolling, cold rolling, primary annealing, and secondary annealing. Furthermore, experiments are described in which the evolution of a Goss-oriented single crystal was tracked during the cold rolling and primary annealing in order to gain more information on the origin of abnormal Goss grain growth. All observations the of microstructure and microtexture were carried out by means of a high resolution and high speed EBSD (electron backscatter diffraction) analysis system (TSL OIM software; JEOL 6500F field emission gun scanning electron microscope) that allows to map very large areas, in order to detect the very rare Goss grains, as well as to precisely reconstruct the microstructure of heavily deformed samples.

2. Microstructure and microtexture evolution

2.1. Hot rolling

Industrial material: During hot rolling the Goss orientation originates due to shear deformation close to the strip surface [1–5]. Our microtexture measurements revealed some quite large Goss grains without visible substructure (Fig. 1). However, other Goss grains are much smaller, reveal a substructure or an orientation gradient.

Single crystal experiments: The idea of our single crystal experiments is visualized in Fig. 2: we grabbed one of the Goss grains in the hot rolled material and deformed and

*Corresponding author. Tel.: +49 211 6792 803.
E-mail address: zaefferer@mpie.de (S. Zaefferer).

0304-8853/$ - see front matter © 2006 Elsevier B.V. All rights reserved.
doi:10.1016/j.jmmm.2006.02.116

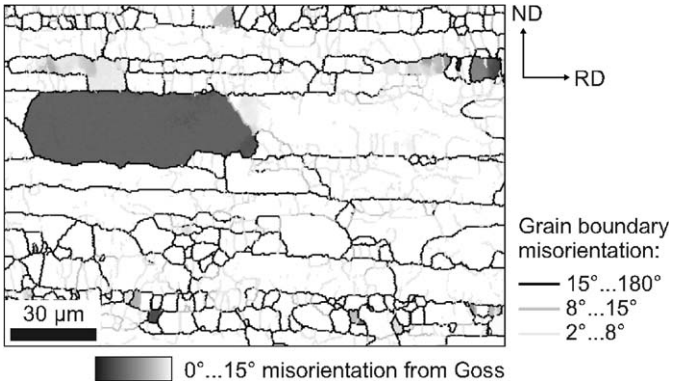

Fig. 1. Large Goss grain in industrially hot rolled silicon steel. Crystal orientation map including grain boundaries. RD: rolling direction; ND: normal direction.

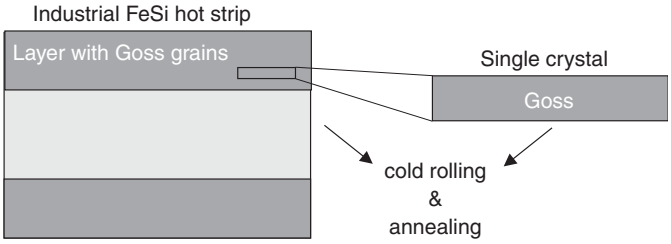

Fig. 2. Idea of single crystal experiments.

annealed it in the same way as it was done with the industrial polycrystalline silicon steel. Experimentally this was done by growing a macroscopic Goss-oriented single crystal ($20 \times 50 \times 2.2\,mm^3$) which was then used for cold rolling [6,7] and annealing experiments.

2.2. Cold rolling

Industrial material: As already known from earlier studies on industrially cold rolled silicon steel, the major texture components after cold rolling are the α-fibre and the γ-fibre [1,8,9,4]. However, our microtexture measurements revealed that small Goss-oriented areas are also present in the cold rolled microstructure. The area fraction of the Goss orientation is about 1% taking into account a maximum misorientation from exact Goss of 15°. This weak Goss component was not detected in earlier studies due to the lower resolution of the X-ray diffraction compared to the EBSD technique. Furthermore, we observed that the occurrence of Goss-oriented areas was restricted to regions with orientations close to $\{111\}\langle 1\,1\,2\rangle$ (Fig. 3). Most of the Goss grains were aligned along shear bands, however, very few Goss grains appeared to occur in less strained areas outside of shear bands.

Single crystal experiments: Cold rolling of a Goss-oriented single crystal resulted in a crystal rotation into the two symmetrically equivalent $\{111\}\langle 1\,1\,2\rangle$ texture components as already reported by Dunn [10]. But we found that Goss-oriented areas were still present in the

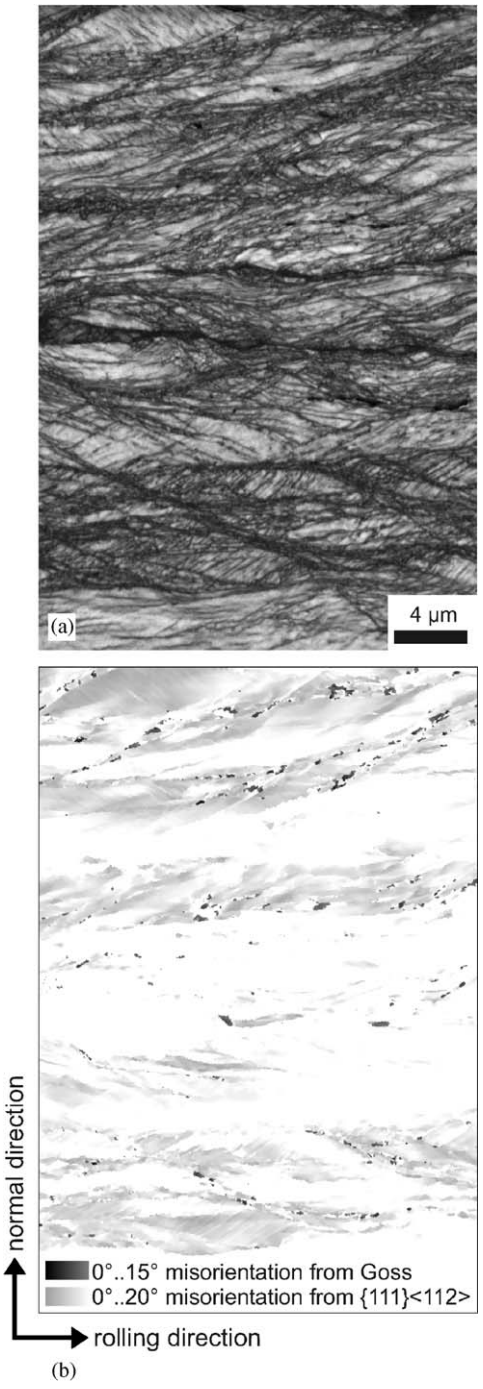

Fig. 3. Industrial silicon steel: (a) Microstructure with characteristic shear bands. EBSD pattern quality map: darker areas represent a higher dislocation density; (b) Crystal orientation map. The Goss-oriented areas occur only next to $\{111\}\langle 1\,1\,2\rangle$-oriented areas.

highly strained material with a fraction of 2.2–2.6%, although the Goss orientation is not stable under plane strain deformation [9,11]. In particular, we observed two types of Goss grains (Fig.4). Goss grains inside of shear bands newly formed during deformation at high strain. Whereas we supposed that those Goss grains that were found between microbands were retained during cold rolling [6,7].

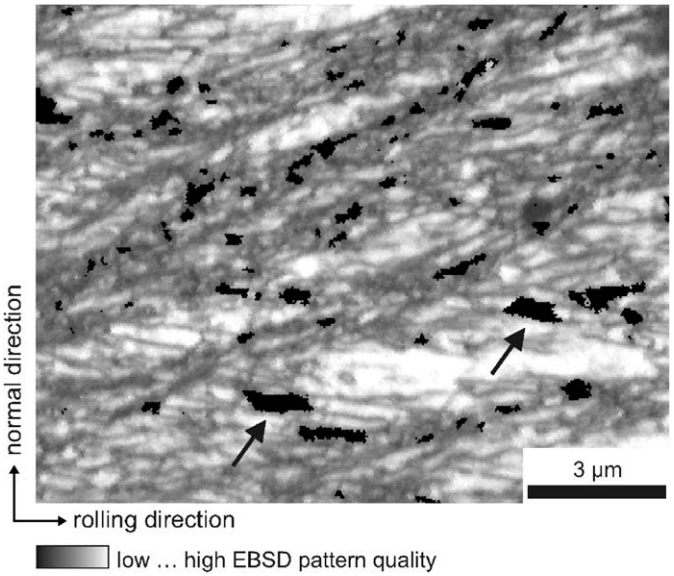

Fig. 4. Single crystal experiments. Goss-oriented areas in a 89% deformed, originally Goss-oriented single crystal. The Goss grains are situated both inside of shear bands and between microbands (arrows). EBSD pattern quality map; Goss-oriented areas are marked in black.

2.3. Primary annealing

Industrial material: After primary recrystallization the Goss orientation forms a minor texture component in high permeability grade material and is a one of the main texture components in conventional grade silicon steel. In both grades, the major texture component is the γ-fibre e.g. Ref. [3]. Microtexture analysis showed that the Goss grains are not larger than other grains, i.e. they do not have a size advantage during secondary annealing [12].

Single crystal experiments: In contrast to the industrially processed material, in the deformed and annealed originally Goss-oriented single crystal, the Goss orientation is the strongest texture component. Our microstructure analysis revealed that the Goss grains between the microbands are likely to form nuclei for primary recrystallization. The Goss grains inside of shear bands mostly disappeared.

2.4. Secondary annealing

Industrial material: During the final high temperature annealing, normal grain growth is inhibited by particle pinning of grain boundaries e.g. Ref. [3]. However, some of the Goss grains that are present in the primary recrystallized material can unpin and grow abnormally giving rise to the formation of a sharp and strong Goss texture.

3. Origin of abnormal Goss grain growth

Abnormal Goss grain growth can be due to a growth selection or an oriented nucleation mechanism. Most existing models of abnormal Goss grain growth propose a growth selection mechanism based on special grain boundary properties, that are e.g. the $\Sigma 9$ grain boundary theory [13,14] or the high angle grain boundary theory [15]. However, these theories cannot explain all experimental observations on abnormal Goss grain growth as it was recently outlined by Zaefferer and Chen [16]. Thus, we assume that there is another, probably an oriented nucleation mechanism leading to abnormal Goss grain growth. We suspect that the Goss grains are characterized by a special microstructure, e.g. dislocation structure, which originates in the early production stages and is inherited through the production process. Our search for special microstructural properties of Goss grains is facilitated by the use of single crystals as the starting material, because in this case the number of Goss grains is higher in the cold rolled and in the primary recrystallized states.

4. Discussion

Our EBSD investigations rendered possibly a detailed analysis of the microstructure and microtexture of particularly the deformed state of silicon steel. We found that in the cold rolled industrial material Goss-oriented areas only occurred in the neighborhood of $\{111\}\langle 1\,1\,2\rangle$ grains. This observation implied that findings from our single crystal experiments, where the texture components were only Goss and $\{111\}\langle 1\,1\,2\rangle$, can possibly be transferred to polycrystalline material. In the industrial material, most of the Goss grains were aligned along shear bands, but some appeared not to be related to shear bands. This was consistent with our observation on the originally Goss-oriented single crystal material. In this case after deformation two types of Goss grains were found: in shear bands and between microbands. The Goss grains in shear bands newly developed during deformation. Whereas those between microbands were retained during cold rolling. Their primary recrystallization behaviour was also different. The Goss grains between microbands formed the recrystallisation nuclei, whereas the Goss grains in the shear bands mostly disappeared during annealing. This observation is in contrast to that of Ref. [8] who stated the formation of new Goss-oriented crystals in shear bands. This indicates that possibly some ideas about the formation of Goss grains have to be revised.

5. Summary

In this study the evolution of the microstructure and microtexture of silicon steel was investigated using EBSD. In particular the development of the Goss orientation was tracked in both industrial material and single crystal material. A study on the evolution of the Goss orientation throughout all production stages is important with regard to the question of the origin of abnormal Goss grain growth, because the Goss orientation originates during hot rolling and is inherited to the final secondary annealing. For the industrial material, we found that the occurrence and the amount of the Goss orientation is related to the

{111}⟨1 1 2⟩ orientation. The most important finding for the single crystal was that two types of Goss grains occurred in the cold rolled state, which also showed different primary recrystallization behaviour. We supposed that results obtained from single crystal experiments can be transferred to industrial material and that they offer the potential to investigate the microstructure of individual Goss grains helping to solve the question of the origin of abnormal Goss grain growth.

Acknowledgment

Financial support by ThyssenKrupp Electrical Steel GmbH is gratefully acknowledged.

References

[1] A. Böttcher, K. Lücke, Acta Metall. Mater. 41 (1993) 2503.
[2] M. Matsuo, T. Sakai, S. Yozo, Metall. Trans. 17A (1986) 1313.
[3] M. Matsuo, ISIJ Int. 29 (1989) 809.
[4] S. Mishra, C. Därmann, K. Lücke, Metall. Trans. 17A (1986) 1301.
[5] Y. Shimizu, Y. Ito, Y. Iida, Metall. Trans. 17A (1986) 1323.
[6] D. Dorner, L. Lahn, S. Zaefferer, Textures of Materials—ICOTOM, vol. 14, pp. 1061, Trans Tech Publ. 2005.
[7] D. Dorner, S. Zaefferer, D. Raabe, Acta Mater., in revision.
[8] T. Haratani, W.B. Hutchinson, I.L. Dillamore, P. Bate, Metal Sci. 18 (1984) 57.
[9] M. Hölscher, D. Raabe, K. Lücke, Steel Res. 62 (1991) 567.
[10] C.G. Dunn, Acta Metall. 2 (1954) 173.
[11] D. Raabe, Z. Zhao, S.-J. Park, F. Roters, Acta Mater. 50 (2002) 421.
[12] N. Chen, S. Zaefferer, L. Lahn, K. Günther, D. Raabe, Acta Mater. 51 (2003) 1755.
[13] H. Homma, B. Hutchinson, Acta Mater. 51 (2003) 3795.
[14] T. Nakayama, Y. Ushigami, Mater. Sci. Forum 47 (1992) 413, 94.
[15] Y. Hayakawa, J.A. Szpunar, Acta Mater. 45 (1997) 4713.
[16] S. Zaefferer, N. Chen, Solid State Phenomena 29 (2005) 105.

Materials Science Forum Vols. 408-412 (2002) pp 949-954
online at http://www.scientific.net

Abnormal Grain Growth in Silicon Steel

N. Chen[1], S. Zaefferer[1], L. Lahn[2], K. Günther[2] and D. Raabe[1]

[1] Max-Planck-Institute for Iron Research, Max-Planck-Strasse 1, DE-40237 Düsseldorf, Germany

[2] Thyssen Krupp Electrical Steel R&D Department, Kurt-Schumacher-Str. 95, DE-45881 Gelsenkirchen, Germany

Keywords: Abnormal Grain Growth, EBSD, Grain Boundary Mobility, Monte Carlo Simulation, Si Steel

Abstract. Grain growth during secondary recrystallization of polycrystalline materials is controlled by driving force and grain boundary mobility. Experiments and simulations have been carried out to sort out which of these effects are responsible for the development of the sharp Goss texture during secondary recrystallization of Si-steel. The influence of surface energy and chemical composition difference as driving force for abnormal Goss grain growth has been investigated by EBSD measurements. In modeling of abnormal grain growth by a Monte Carlo method, mobility of CSL grain boundaries and high energy grain boundaries have been checked using EBSD measurement results as initial microstructure. The real orientation distribution of the material has been taken into account.

Introduction

Understanding of the texture selection mechanism in the abnormal grain growth in grain oriented silicon steel is crucial for the optimization of the production process and the quality improvement of the product. Unfortunately, details of the phenomenon are still not clear. Two mechanisms for the development of secondary recrystallization Goss texture have been frequently considered in the literature. The first one suggests that the boundaries of Goss oriented grains are more frequently of a special coincidence site lattice (CSL) type than that of other grains and that these CSL boundaries are, in the presence of precipitates, more mobile than general boundaries [1,2]. Goss grains therefore have a growth advantage. The second view [3,4] is based on the assumption that the high mobility is a feature of high-energy boundaries (boundaries with misorientation angles between 20 to 45 degrees). Actually, Goss grains in electrical steels are surrounded by the highest proportion of high energy boundaries, thus their growth rate should be faster than that of all other grains. Both of these two theories take the grain boundary mobility difference as reason for abnormal Goss grain growth and the grain boundary energy as its driving force .

Generally, it is difficult to measure the mobility distribution of different types of grain boundaries directly, and a lot of bicrystals with different misorientation relationships would be necessary for this measurement. Moreover, in Si-steel the mobility of a grain boundary is affected by the inhibitor coarsening process, which makes the mobility distribution more complicated. Therefore, recently Monte Carlo type simulations [5] have frequently been used to investigate the grain growth process, and by this method the different mobility distribution can be easily checked. In this paper this method has been used to examine the different grain boundary mobility hypotheses. By a comparison with experimental result it was checked whether the hypothesis might be correct or not.

Generally, grain boundary migration velocity is expressed as :

$$v = mf \qquad (1)$$

where m is defined as the mobility of a grain boundary and f is the driving force responsible for the grain boundary migration. A higher velocity of a Goss grain boundary can thus be obtained by

either a higher mobility of Goss grain boundaries or a lower volume energy of the Goss grains. Various sources of driving forces are tabulated in Tab.1 [6]. Deformation energy may be excluded because the process occurs in a recrystallized matrix. Size advantage of Goss grains at the early stage of secondary recrystallization (with the grain boundary energy as driving force) is uncertain due to a lack of experimental support [7] and due to our own simulation results. Therefore, some experiments have been carried out to check the importance of the other two possible driving forces, the surface energy and a chemical driving force.

Driving force type	Deformation energy	Grain boundary energy	Surface energy	Chemical driving force
Estimated driving force [MPa]	10	10^{-2}	2×10^{-4}	6×10^{2}

Tab. 1. Different types of driving forces for grain boundary migration

Experiments and Simulation

Grain-oriented silicon steel sheets with MnS as inhibitor, produced by two-stage cold-rolling were investigated. After decarburization different samples were heated up to 1173K (Sample A) and 1193K (Sample B), respectively, under hydrogen atmosphere and cooled down to room temperature in the furnace. After this heat treatment the specimens showed a partially secondary recrystallized structure which was studied in the SEM using electron backscatter diffraction (EBSD) and energy dispersive x-ray spectroscopy (EDX). The measurements were carried out in a JEOL 6500F field emission gun SEM.

Another sample showing a fully primary recrystallized structure (after decarburization) was used to give a start microstructure for the simulation study: The EBSD data measured with 1 μm step size were remapped into a Monte Carlo potts model. Using this method the genuine orientation distribution of the material was considered in the Monte Carlo simulation. Simulation was performed on a 1200×1200 sites, fully periodic square lattice with first and second neighbor interaction. The total number of grains in the initial microstructure was 852.

The Monte Carlo model used here has been described in literature [5] in theoretical and computational detail. In this model grain boundary energy is related to misorientation angle of grain boundaries. According to some experimental data, Hayakawa and Szpunar [3] proposed a fitting function to express the relationship between grain boundary energy and misorientation angle in Si steel. A similar expression of grain boundary energy as a function of misorientation angle was used in this paper:

$$\gamma(\theta)=\begin{cases} E_0\theta[A-\ln\theta] & \theta<\theta_m \\ E_0\theta_m[A-\ln\theta_m]-k(\theta-\theta_m) & \theta\geq\theta_m \end{cases}. \qquad (2)$$

γ is the grain boundary energy, θ is the misorientation angle and E, A, k, θ_m are constants. In this paper, calculated from a fitting procedure, A is 0.234, k is 0.005 and θ_m is 40 degrees.

One purpose of the study was to check whether a higher mobility of CSL grain boundaries or of high-energy boundaries is responsible for abnormal Goss grain growth. For this reason, two hypotheses of grain boundary mobility distribution were investigated in this simulation.

The first hypothesis (*1*) is that CSL grain boundaries (especially $\Sigma5$, $\Sigma7$ and $\Sigma9$) have higher mobility than others. According to the Brandon criterion [8], misorientations with angular deviations of less than $\delta\theta_{\Sigma}=15^{o}/\Sigma^{1/2}$ degrees from the precise CSL misorientation are within the CSL grain boundary. Using a Read-Shockley model [9], the normalized CSL grain boundary mobility is given by:

$$M(\theta) = M_0 + \frac{k}{\sum}\left\{1 - \frac{\delta\theta}{\delta\theta_{\sum}}\left[1 - \ln\left(\frac{\delta\theta}{\delta\theta_{\sum}}\right)\right]\right\}. \quad (3)$$

Here M_0 and k are constants, and in this paper, M_0 is set to 0.5 and k is set to 2.7. $\delta\theta$ is the deviation angle between a grain boundary and a precise CSL grain boundary. It is calculated by :

$$M_m = M_g M_{CSL}^{-1}, \quad (4)$$

where M_g is the misorientation matrix of the grain boundary and M_{CSL} is the misorientation matrix corresponding to the precise CSL grain boundary.

The second hypothesis (*2*) of mobility distribution is that high-energy grain boundaries have higher grain boundary mobilities. To simulate this, the simple assumption that relative grain boundary mobility is proportional to its grain boundary energy is used in this paper. The grain boundary energy and grain boundary mobility distributions used in the different hypotheses are presented in Fig.1.

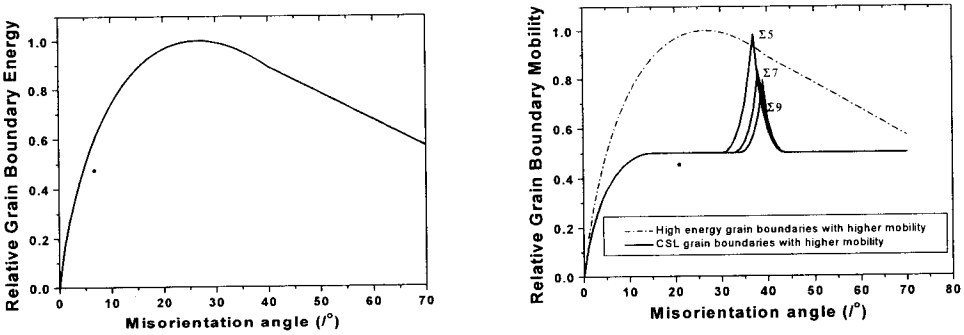

(a) Grain boundary energy (b) Grain boundary mobility

Fig. 1. Grain boundary energy and grain boundary mobility used in the MC simulation

Results and Discussion

From Tab.1 it can be seen that besides grain boundary energy, surface energy and chemical potential are possible driving forces for abnormal Goss grain growth in the secondary recrystallization of Si-steel. Kramer [10] found that the surface energy of Si-steel is sensitive to the atmosphere and under hydrogen atmosphere the surface energy of {110} is lower than that of other planes. A Goss grain located in the surface area of a sample could therefore have an extra driving force for grain growth given by the surface energy.

EBSD results of samples A and B are shown in Fig.2, In sample A one Goss grain is very large, but has not yet penetrated all sample thickness, while in sample B, the Goss grain has penetrated the whole thickness and grows only in the direction within the sheet plane. If the surface energy would be the driving force for abnormal Goss grain growth, the grain boundary of the Goss grain located in the surface should have higher migration velocity due to the higher driving force compared to the Goss grain boundary in the interior of the sample, which is in contrast to the observation in figure 2. Here the fastest growing area of the Goss grain is, in fact, not at the surface of the sample but in its interior. This behavior might be caused by a misorientation-dependent grain boundary mobility. It can thus be concluded that during secondary recrystallization surface energy does not play the most important role for abnormal Goss grain growth.

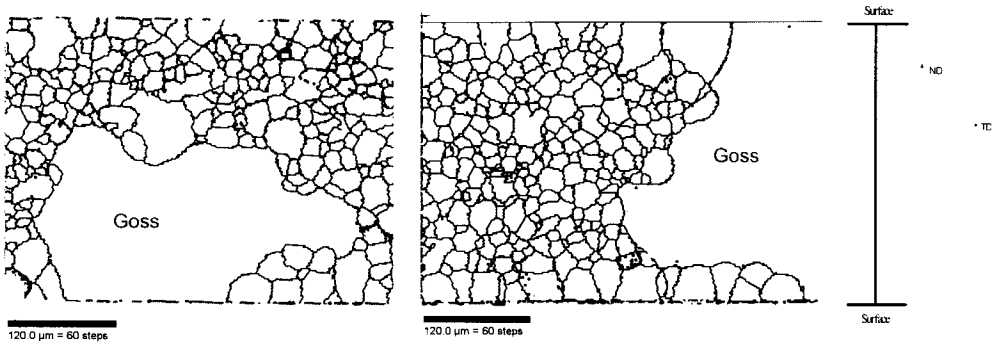

(a) Sample A (1173K) (b) Sample B (1193K)

Fig. 2. EBSD result of sample A and sample B

Recently, it has been indicated that during the initial stage of secondary recrystallization of Si steel grains grow slowly and uniformly, until, after a specific time, suddenly Goss grains grow rapidly and within 1 or 2 min Goss grain size is increased from about 20-30 µm to 1mm or more [11]. During this period, migration velocity of Goss grain is very high and Suzuki et al. [12] found that the migration velocity of Goss grain boundary is about 10 µm /sec at 1293K.

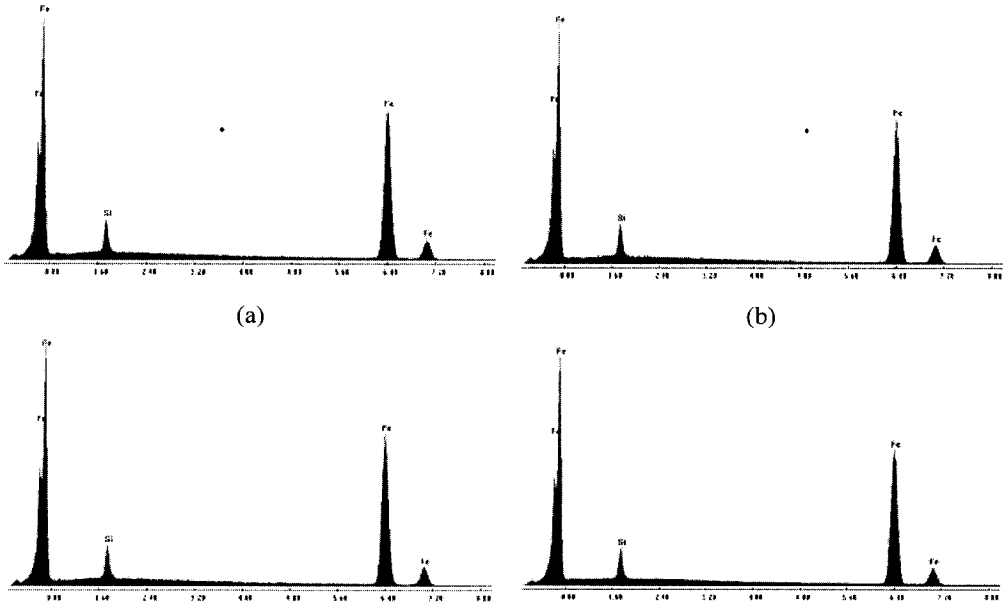

(a) (b)

(c) (d)

Fig. 3. Chemical composition in different area of growing Goss grain and its neighbor grains (non-Goss orientation) (a) Goss interior (b) Goss near boundary (c) Non-Goss grain interior (d) Non-Goss near grain boundary

According to Eq.(1) the mobility of Goss grain boundary or driving force for Goss grain growth should be enormous. From Tab.1, the largest driving force for grain boundary migration is chemical driving force, which generally occurs during phase transformation processes. To check for any influence of chemical composition EDX measurements of the chemical composition were carried out in different areas of sample B: inside the Goss grain in its center and close to its grain boundary and inside a non-Goss grain also in its center and close to the grain boundary. All results are shown

in Fig.3 and it is clear that chemical composition in different areas is almost the same and that a difference in chemical composition is not the driving force for abnormal Goss grain growth.

The grain boundary distribution obtained from EBSD data in the primary recrystallized state is presented in Fig.4. It can be seen that the fraction of CSL grain boundaries is very low (area fraction of $\Sigma 5$, $\Sigma 7$ and $\Sigma 9$ grain boundaries are 2.2%, 0.7% and 0.9%, respectively), while the area fraction of high-energy grain boundaries (47.8%) is very high. From figure 5a it can be seen that after primary recrystallization the Goss grain fraction is very low (2%) and the average grain size of Goss grains is 20.2 μm, while the average grain size of all grains is 22.4 μm.

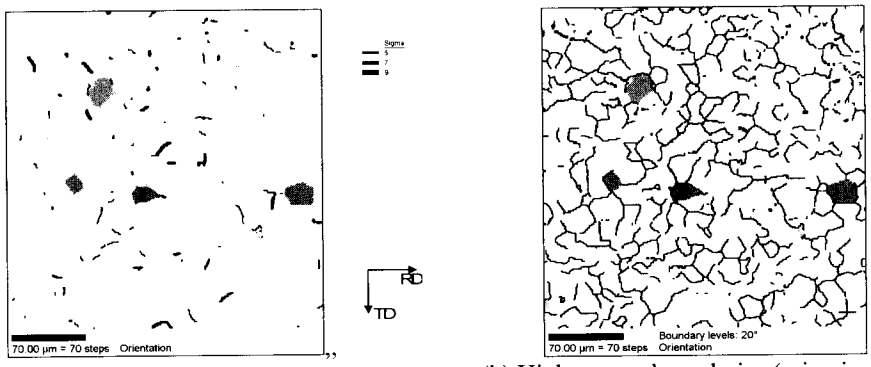

(a) CSL grain boundaries defined by Brandon criterion

(b) High energy boundaries (misorientation angle between 20-45 degree)

Fig.4. Grain boundary distribution in recrystallized Si-steel

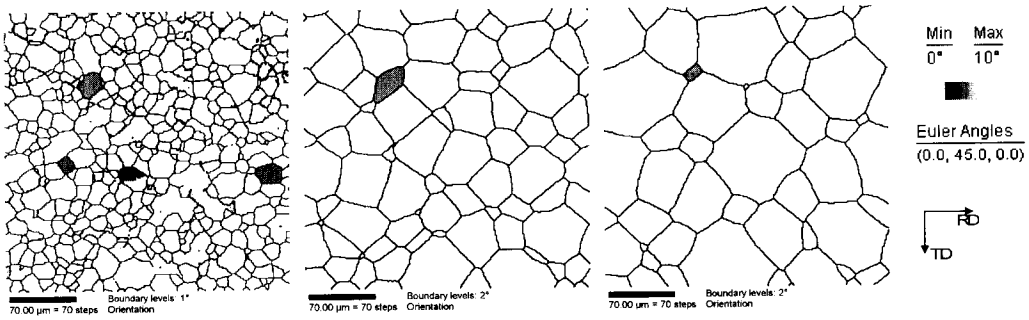

(a) Orientation map

(b) Simulation with hypothesis 1 MCS=40000

(c) Simulation with hypothesis 2 MCS=40000

Fig.5. Orientation map (EBSD) and result of simulation (after primary recrystallization, dark areas are corresponding to Goss grains) MCS = Monte-Carlo Steps

Figures 5 and 6 show the microstructures and pole figures from the measurement and from the simulations using the different hypotheses 1 and 2. The average grain size of fig.5b is smaller than that of fig.5c. This can be easily understood from the fact that in hypothesis 1 the CSL grain boundaries have high mobility while in hypothesis 2, high energy grain boundaries - of which there are much more after primary recrystallization - have high mobility. The second hypothesis therefore leads to a larger average grain boundary velocity and therefore to a larger average grain size for the same MCS value. Both simulation hypotheses do not lead to any preferred growth of the Goss

grains. Actually, according to hypotheses 1 Goss grains should have more CSL grain boundaries than other grains, which is, however, not observed in the experiments (see Fig. 4a). More over, this theory cannot explain why there are no crystals with other orientation showing abnormal grain growth although there are grains of non-Goss orientation with CSL grain boundaries. Finally, it is also not clear, how the misorientation between two grains could be sharply related to the rolling process, which is, however, certainly the case for the growing Goss grains. Concerning the second hypothesis, there are a lot of high-energy grain boundaries with high mobility in the matrix, leading to many grains that can grow rapidly. This is contradicted by the fact that in the initial stage of abnormal grain growth only few grain boundaries are involved in abnormal grain growth.

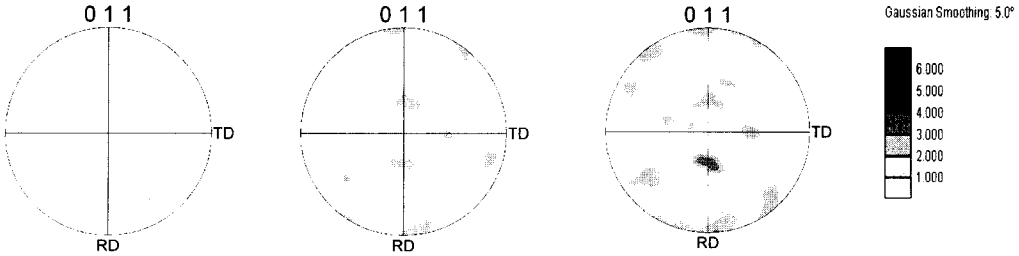

(a) Pole figure from EBSD measurements (max.=3.40)

(b) Pole figure of simulation result (CSL grain boundaries with higher mobility) (max.=4.25)

(c) Pole figure of simulation result (High angle grain boundaries with higher mobility) (max.=5.13)

Fig.6. Pole figure of EBSD measurement result and simulation result

Anyway, the shape of the Goss grains in figures 2a and 2b shows that grain boundary mobility with different misorientation must be different. However, as our experimental and simulation results suggest, the misorientation-dependent grain mobility cannot be the sole reason for abnormal Goss grain growth.

Summary

1. Neither Surface energy nor chemical driving force is the main driving force for abnormal grain growth of Goss.
2. Misorientation-dependent grain boundary mobility is not the sole reason for abnormal Goss grain growth from our experimental and simulation results.

References

[1] R.Shimizu and J.Harase: *Acta Metall.* 37, (1989) p.1241
[2] P.Lin, G.Palumbo, J.Harase, and K.T.Aust: *Acta Mater.* 44, (1996) p.4677
[3] Y.Hayakawa and J.A.Szpunar: *Acta Mater.* 45, (1997) p.1285
[4] N.Rajmohan, J.A.Szpunar and Y.Hayakawa: *Acta Mater.* 47, (1999) p.2999
[5] N.Ono, K.Kimura and T.Watanabe: *Acta Mater.* 47, (1999) p.1007
[6] G.Gottstein and S.Shvindlerman: "*Grain Boundary Migration in Metals*", CRC Press, 1999
[7] A.Morawiec : *Scripta Mater.* 43, (2000) p.275
[8] D.G.Brandon, *Acta Metall.*, 14, (1966) p.1479
[9] A.P.Sutton and R.W.Balluffi, "*Interfaces in crystalline materials*", Oxford Science publications; Oxford, U.K., 1995
[10] J.J.Kramer, *Metal.Trans.A*, 23A, (1992) p.1987
[11] K.Günther etc, Scientific Report of Thyssen Krupp, 2000
[12] S.Suzuki,Y.Ushigami,H.Homma,S.Takebayashi and T.Kubota, *Mater.Trans.* 42, (2001) p.994

Textures of Materials - ICOTOM 13
doi:10.4028/www.scientific.net/MSF.408-412

Abnormal Grain Growth in Silicon Steel
doi:10.4028/www.scientific.net/MSF.408-412.949

Available online at www.sciencedirect.com
SCIENCE DIRECT®
Pergamon
Acta Materialia 51 (2003) 1755–1765
Acta MATERIALIA
www.actamat-journals.com

Effects of topology on abnormal grain growth in silicon steel

N. Chen [a,*], S. Zaefferer [a], L. Lahn [b], K. Günther [b], D. Raabe [a]

[a] *Max-Planck-Institut für Eisenforschung, Max-Planck-Str. 1, D-40237 Düsseldorf, Germany*
[b] *ThyssenKrupp Electrical Steel R&D Department, Kurt-Schumacher-Str. 95, D-45881 Gelsenkirchen, Germany*

Received 26 July 2002; received in revised form 7 November 2002; accepted 30 November 2002

Abstract

This work addresses the role of grain topology on abnormal grain growth in silicon steel. The question was investigated whether the abnormal grain growth of Goss grains during secondary recrystallization can be interpreted in terms of an initial size advantage that these grains inherit from rolling and primary recrystallization. For this purpose the correlation between crystallographic orientation, size and number of next neighbors of large grains in the subsurface layer of a primary recrystallized silicon steel sheet was investigated. It was found that most of the large grains have an orientation on the η-fiber ($<001>$ axis parallel to the rolling direction) but are not particularly close to the Goss orientation. Also, no tendency of grains to be larger the closer they are to the Goss orientation was visible. Rather it was found that the scatter of the angular deviation to the Goss orientation is similar over a large range of grain sizes and this was found to be true too if the number of next neighbors of a grain rather than its grain size was checked. One single grain, however, was found that was close to the Goss orientation and had a high number of next neighbors and might therefore act as a nucleus for secondary recrystallization. Nevertheless, grains with a similarly high number of neighbors and a large deviation to the Goss orientation were found, too. Thus, a topological reason for the Goss texture evolution could not yet be proved. However, it might be that the extreme rareness of Goss nuclei (1 out of 10^6 grains) has prevented, up to now, from observing a true nucleus.

Keywords: Grain growth; Texture; Grain topology; Silicon steel; Goss grains

1. Introduction

The pronounced formation of large grains with a $\{110\}<001>$ crystal orientation during annealing of silicon steel sheets has been extensively investigated since the early work of Goss [1], Ruder [2], and Burwell [3]. The occurrence and orientational sharpness of the $\{110\}<001>$ texture component which is also referred to as Goss orientation is of considerable interest both from a technological and from a scientific point of view. The strong Goss texture which develops by secondary recrystallization can be very sharp although it does not prevail in the texture of primary recrystallized Si steel sheet.

* Corresponding author. Tel.: +49-2116-79-2800; fax: +49-2116-79-2333.
E-mail address: chen@mpie.de (N. Chen).

1359-6454/03/$30.00
doi:10.1016/S1359-6454(02)00574-8

As primary recrystallization, secondary recrystallization is a process of nucleation followed by grain growth. The driving force for this process is the reduction of grain boundary energy. As in primary recrystallization, the secondary recrystallization texture formation may be explained by one or both of the two competing models of *oriented nucleation* and *oriented growth*. In contrast to primary recrystallization, however, secondary recrystallization, or abnormal grain growth, stands in competition with the process of normal grain growth, which also leads to a reduction of the grain boundary energy. Abnormal grain growth can only proceed if normal grain growth is inhibited. The inhibition occurs in most cases by finely dispersed particles which pin the grain boundaries. For this case Hillert [4] has shown how particle size and distribution influence the critical grain size necessary for nucleation of secondary recrystallization. In other cases the inhibition of normal grain growth may occur by the existence of a very sharp primary texture. In this case the low angle grain boundaries between most of the grains prevent normal grain growth and only those grains with strongly deviating orientations may grow abnormally. It should be mentioned that in the case of polycrystals which do not contain any second-phase particles and show a random texture large grains will always grow more slowly than small grains and will finally join the normal grain size distribution [4,5]. Thus, in such 'ideal' polycrystals abnormal grain growth will never occur.

In the case of the Goss texture formation in primary recrystallized silicon steel the inhibition of normal grain growth occurs by particles (manganese sulfide or aluminum nitride particles), while texture has no serious inhibiting effect because the primary recrystallization texture is rather weak. This has already been shown by investigations of May and Turnbull [6] on high purity silicon steel where no abnormal grain growth occurred because second phase particles were absent.

Concerning the mechanism of texture formation the idea of oriented growth has been most frequently favored and two models have been proposed. The first one [7,8] suggests that CSL (coincidence site lattice) grain boundaries are responsible for the abnormal growth of Goss grains. Statistically, Goss oriented grains in a typical primary recrystallization texture have a higher probability than other orientations to form low-Σ CSL boundaries (i.e. boundaries with a high number of lattice coincidence sites). Lin et al. [8] claimed that these boundaries have a higher mobility than others. It should be noted in this context that the CSL model has no physical meaning as such but is a geometrical concept from which possible physical mechanisms such as grain boundary dislocations or solubility of foreign atoms can be derived.

The second view on oriented growth of Goss grains is based on the assumption that high mobility is a feature of high-angle boundaries with misorientation angles between 20 to 45° [9,10]. The idea here is that the high diffusivity of these boundaries leads to quick coarsening of precipitates during annealing. The resulting large particles have a lower pinning force on the moving boundaries than smaller particles on other boundaries. Goss grains have been reported to be surrounded by a higher fraction of these high mobility grain boundaries than grains with other orientations. This unique configuration is assumed to be the reason for abnormal growth of Goss grains.

Both approaches have recently been discussed by Morawiec [11] who concluded that possible differences in grain boundary mobility might not be the sole reason for the abnormal grain growth of Goss grains. Using local orientation measurements and Monte Carlo simulations Chen at al. [12] also found that differences in the mobility alone do not seem to be sufficient for abnormal grain growth of Goss oriented crystals. Also, it is questionable whether the only statistical link between the Goss orientation and a particular grain boundary character (high angle or CSL grain boundary) is able to create a texture as sharp as the observed Goss texture.

A strong objection against either of these two theories of oriented growth is that usually only very few grains with a sharp Goss orientation are observed to start growing in the early stage of secondary recrystallization, i.e. that there is no growth competition. This observation supports the classical idea of oriented nucleation as main mechanism

of secondary recrystallization. In this case it is assumed that a grain may grow abnormally if it has a certain size advantage over the other crystals in the primary recrystallized matrix. The open problems in understanding this phenomenon are first to define the critical grain size from which on a grain may grow abnormally and second to explain how grains of a sufficient size develop in the matrix. According to Hillert [4] the critical grain size depends on the grain boundary energy, on the average grain size and on the size and distribution of the inhibiting particles. It may also be influenced by the surface energy in case that the grain is close to the free surface of the sheet. The question how a grain may reach the critical grain size has been answered in different ways. Some authors (Matsuo [13], Inokuti et al.[14]) claim the existence of large Goss oriented grains in the primary recrystallized matrix. Matsuo [13] found many Goss grains in the subsurface layer of a hot rolled silicon steel sheet. On the basis of this observation he assumed the presence of some larger Goss grains in this layer also after cold rolling and subsequent primary recrystallization. Others assume that Goss grains may be formed by coalescence of closely oriented grain clusters [Inokuti et al. [14]]. In both cases nuclei for secondary recrystallization are assumed to be created by inheritance from the hot rolled sheet.

Instead of using the grain size as a measure for a topological advantage of a grain it is, according to von Neumann [15], Mullins [16], and Hillert [4], more sensible to use the number of next neighbors of a grain. For the simple case of a two-dimensional microstructure, a grain will grow if it has more than six neighbors and shrink if it has less than six. In the three-dimensional case, no regular polyhedron with plane faces exists which fills space completely and balances the boundary tensions. Therefore, grain growth is inevitable in a three-dimensional microstructure (Smith [17]). However, also in this case the tendency remains that grains with many neighbors grow while those with few shrink. In the case of grains in a microstructure with a homogeneous grain size distribution as it is the case here, however, statistically the number of next neighbors of a grain and the grain size are approximately related by a square function. This means that in a first approximation grain size can be used to discuss the tendency of a grain for grain growth and this approach has been mainly adapted here. Local considerations, in contrast, must be based on the number of next neighbors.

The suggestion of oriented nucleation, i.e. initial size advantage of Goss grains has until now not been systematically investigated by experiment. This is essentially due to the rareness of the nucleation event: assuming a grain size of 20'20'20 μm^3 in the primary recrystallized matrix and of about 2000'2000'200 μm^3 in the secondary recrystallized material (200 μm is the sheet thickness) it is clear that on 106 primary grains comes only one successful Goss grain as nucleus for secondary recrystallization. One therefore must inspect at least 106 grains in order to observe one nucleus. This points out the demand for a fast and efficient method for single grain orientation and grain size measurements.

The aim of the present study, therefore, is to quantitatively investigate the possible existence of a size advantage of Goss-oriented (or any other) grains in the subsurface layer of primary recrystallized silicon steel sheet and to check whether such orientational topology effects might play a role for abnormal grain growth in this material.

2. Experimental

Material used in this investigation was a fully primary recrystallized Fe–3% Si sheet, which was produced by two-stage cold rolling. MnS was used as inhibitor in this type of Si steel. The texture after secondary recrystallization was investigated on a sheet which was secondary annealed by heating it for 40 h up to 1000 °C under H_2 atmosphere.

Automatic crystal orientation mapping (ACOM) was performed in a JEOL 6500F field emission gun scanning electron microscope (FEG-SEM). The ACOM technique allows determination of the crystallographic texture and the microstructure in crystalline material. Local lattice orientations are measured on a regular grid by automated acquisition and processing of electron backscatter diffraction (EBSD) patterns. The microstructure can sub-

sequently be reconstructed by coloring similar orientations on the measured grid with similar colors. The FEG-SEM used in this study is distinguished by its extraordinary high beam current at high resolution. This, together with a high-speed digital CCD camera (DigiView, TSL) for the acquisition of EBSD patterns allows measuring up to 30 patterns per second and enables the measurement of very large orientation maps in an acceptable time span.

Two kinds of investigations were carried out. First, two large orientation maps, covering $2 \times 2 \times 2$ mm^2 were measured with high resolution on the rolling plane in order to detect possible Goss grains and to check for the relationship between texture and grain size. This area contained about 6×10^4 grains. Second, a very large area on the rolling plane of two primary recrystallized samples was investigated by inspection of backscatter electron (BSE) images in order to detect all large grains. To this end two samples with an investigated area of $2 \times 14 \times 24$ mm^2 were used. This area corresponds to about 2×10^6 grains (which were not all investigated by ACOM) and may therefore contain two potential Goss nuclei for the subsequent secondary recrystallization. ACOM measurements were carried out in the areas surrounding all inspected large grains. By this method the orientation and the occupied areas of all large grains were determined. Two rules were used to define what was counted as a *large grain*: First, the grain diameter had to be larger than 40 μm, the average diameter of all matrix grains amounted to about 20 μm. Second, the grain size had to be much larger than that of the immediate neighbor grains.

All ACOM measurements were carried out in the subsurface layer ($s = 0.8$) of the samples in the rolling planes (formed by the rolling direction (RD) and transverse direction (TD)). The parameter s is defined by $s = a/(d/2)$, where a is the distance of the inspected area from the center layer and d the sheet thickness.

From the measured crystal orientations pole figures and orientation distribution functions of the large grains were calculated. For comparison the global texture was calculated from X-ray pole figure measurements carried out with a Siemens D500 X-ray texture goniometer.

The texture results will be discussed in the following in terms of the typical texture fibers found in recrystallized silicon steel. These are namely the α_{bcc}–fiber (fiber axis <110> parallel to the rolling direction including major components {001}<110>, $\{1\bar{1}2\} < 110 >$, and $\{1\bar{1}1\} < 110 >$), the γ–fiber (fiber axis <111> parallel to the normal direction including major components $\{1\bar{1}1\} < 110 >$ and $\{11\bar{1}\} < 112 >$) and the η-fiber (fiber axis <001> parallel to the rolling direction including major components {001}<100> and {011}<100>).

3. Experimental results

Fig. 1 shows the orientation distribution function (ODF) determined by X-ray diffraction. It reveals that the texture in the investigated subsurface layer is dominated by a weak γ-fiber and a texture component on the η-fiber which is about 15° rotated about the rolling direction from the cube orientation. A minor α-fiber component at the 45° rotated cube orientation can also be observed. Fig. 1 also reveals that the exact Goss component is rather weak in the primary recrystallized specimen. Fig. 2 shows the ODF after secondary recrystallization. The texture shows a sharp Goss component with a full width half maximum (FWHM) of about 10°.

The grain size and grain orientation of a large number of grains (about 60 000) was determined by ACOM. The grain size distribution obtained from these measurements is shown in Fig. 3. The average grain size is 17.3 μm and the grain size distribution can be fitted with good precision to the two-parametrical log-normal distribution (Feltham [18]). Naturally, the only one-parametrical Hillert [4] or Rayleigh [19] distributions do not give a similarly good fit.

The correlation between grain size and grain orientation is presented in Fig. 4a in form of a graph which displays for every grain its angular deviation to the exact Goss orientation over its grain size in μm^2. The gray value at each position in the graph corresponds to the number of grains

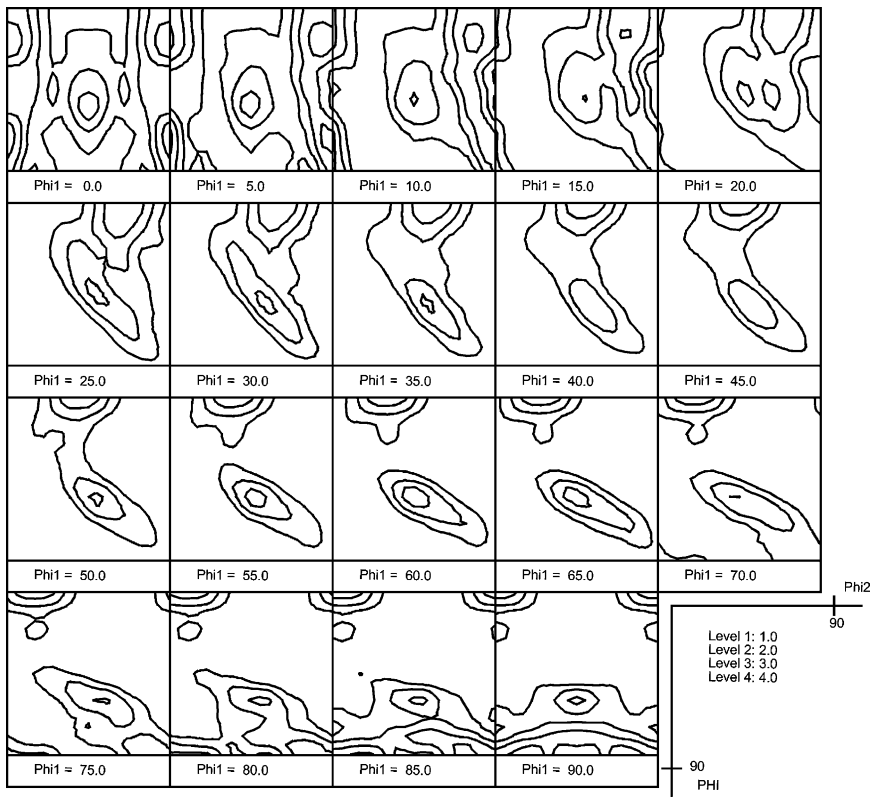

Fig. 1. Orientation distribution function of primary recrystallized silicon steel in the form of φ_1=constant sections using $\Delta\varphi_1$=5° steps between the sections. The texture was determined by measuring the four incomplete pole figures {110}, {200}, {112}, and {103} in the range of the pole distance between 0° and 85° using Mo $K_{\alpha 1}$ x-radiation and deriving the orientation distribution function from it using spherical harmonics. The measurement was conducted in the layer s = 0.8 (see text).

that show similar parameters. It is visible from this graph that some grains have sizes larger than 40 μm but there is no apparent tendency of these grains to be close to Goss orientation. The two solid lines that have been drawn in the graph mark the limit for a possible Goss nucleus with a certain size advantage. The horizontal line indicates an angular deviation of 10° from the exact Goss orientation which corresponds to the observed sharpness of the final texture. The vertical line indicates the grain size of grains which have a diameter two times larger than the average grain size. All grains right and below these lines fulfill the criteria for a Goss grain nucleus. Obviously there are only two grains in this area while several non-Goss oriented grains have large diameters.

As was already mentioned in the introduction the number of next neighbors of a grain is a more sensible measure to evaluate a topological advantage of a grain than the grain size. However, the number of neighbors is more difficult to determine and appropriate algorithms are not included in the commercial ACOM software used here (OIM3 of TSL). Therefore a computer program was developed that determines for every grain in an orientation map the number of next neighbors. An exported data file of the OIM software containing all measurement information (location and orientation of each measurement point) serves as input for the developed algorithm. In a first step, the program uses a recursive algorithm to determine all grains and assign them a unique grain ID. To this end the misorientation of all neighbor points of a given point are checked. If the misorientation angle is less than a predefined value (for example 2°) the neighbor point is considered to be within the same

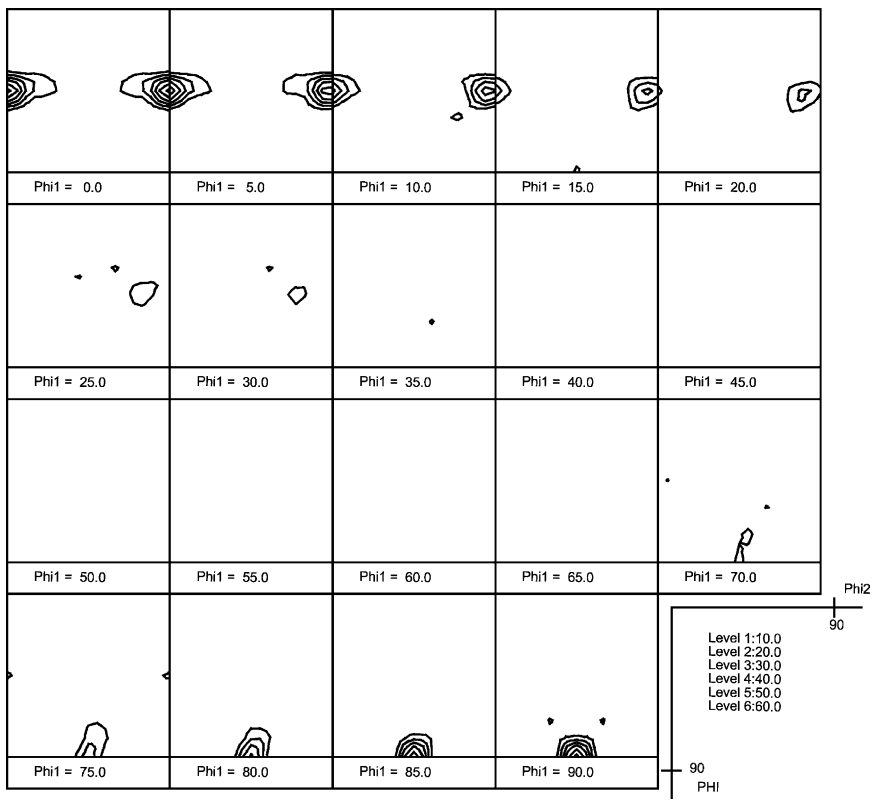

Fig. 2. Orientation distribution function after secondary recrystallization. The measurement parameters are the same as Fig. 1.

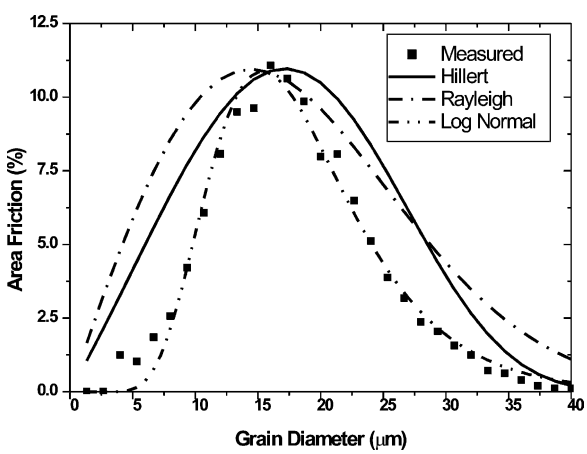

Fig. 3. Grain size distribution determined from ACOM measurements of a large area (4 mm × 2 mm) of a primary recrystallized sample.

grain, otherwise it is in a new grain. In case the point is in the same grain the same algorithm is repeated until all points belonging to one grain are found. After all grains in the OIM map have been detected a second algorithm now simply counts the number of next neighbors of each grain by comparing their grain IDs. The quaternion method is used for the calculation of misorientations in order to speed up the algorithm. On an AMD1000 GHZ computer it takes about 35 s to finish the calculation for a map of 10^6 points. Only some very small grains and grains located on the border of the map are overlooked by the algorithm. The results of these calculations are displayed in Fig. 4b in a similar way as in Fig. 4a. For every grain one point displays its angular deviation to the Goss orientation over its number of next neighbors. The gray value represents the number of grains that fall onto the same position in the graph.

Most grains have less than 13 neighbors with a

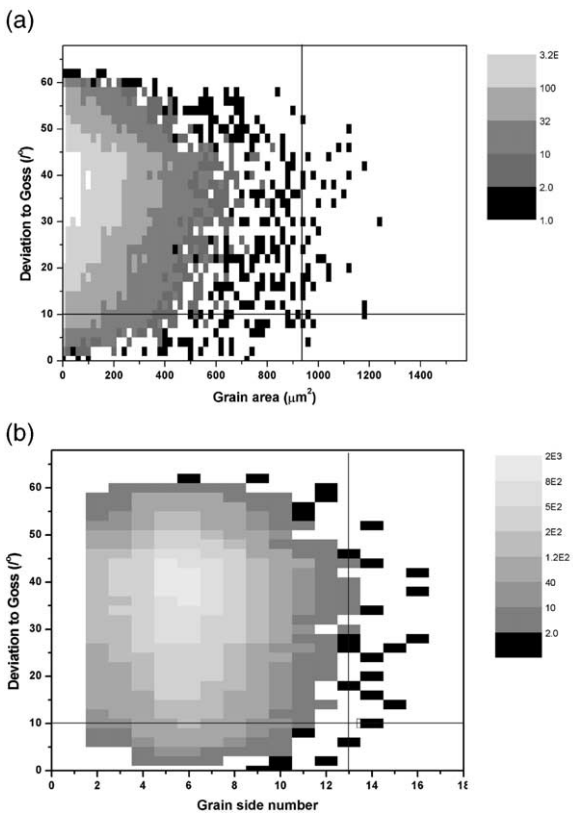

Fig. 4. Correlation between grain topology and angular deviation from the Goss orientation (all data are calculated from an ACOM measurement of a large area (4 mm × 2 mm) of a primary recrystallized sample). The gray value of a given position corresponds to the number of grains that show this particular combination of topology and Goss deviation. Points which correspond to only one single grain are displayed in black on a white background. Do not confuse this background with the white area in the center of the graphic which corresponds to areas with maximum number of grains. (a) Correlation between grain area (in μm^2) and angular deviation to Goss (in °). (b) Correlation between number of next neighbors and angular deviation to Goss (in °).

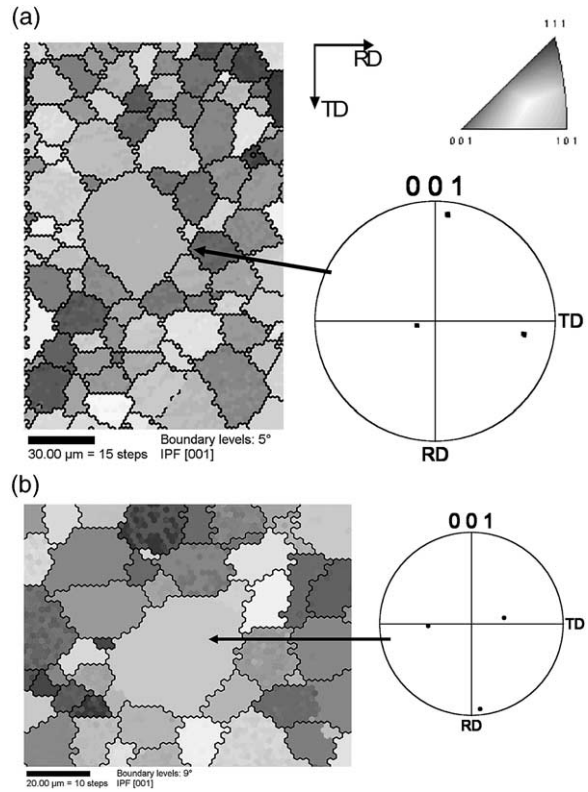

Fig. 5. Crystal orientation maps of large grains in the primary recrystallized silicon steel. The gray value is chosen according to the crystal direction parallel to the normal direction of the sheet. The orientation of the large crystal is displayed as (001) pole figure. (a) Large non-Goss grain on the η-fibre. (b) Goss grain with many neighbors.

maximum of grains owing five or six neighbors as it is expected for a stable two-dimensional structure. The largest number of next neighbors is 16 and there are three grains corresponding to this number. However, their deviation from the Goss orientation is for all of them larger than 25°. There is only one grain with a Goss orientation deviation of less than 10° and a number of next neighbors larger than 14 in this graph. As for the grain size no tendency of grains with a high number of next neighbors to be close to the Goss orientation is visible.

Fig. 5a shows an example of the local orientation measurements that were systematically conducted around all large grains. The pole figure projection shows that this particular grain is close to the cube orientation $\{001\}\langle 100\rangle$. The crystal orientation and size of all inspected 22 large grains are presented in Fig. 6a, the corresponding next-neighbor graph in Fig. 6b. Fig. 6a shows that the area of most of the large grains is in the range between 1200 and 3000 μm^2 corresponding to a diameter of 40–60 μm. The area of the largest grain is 4562 μm^2, i.e. its diameter is about 80 μm which is about four times larger than the average grain size. A comparison between Figs. 6a and 6b

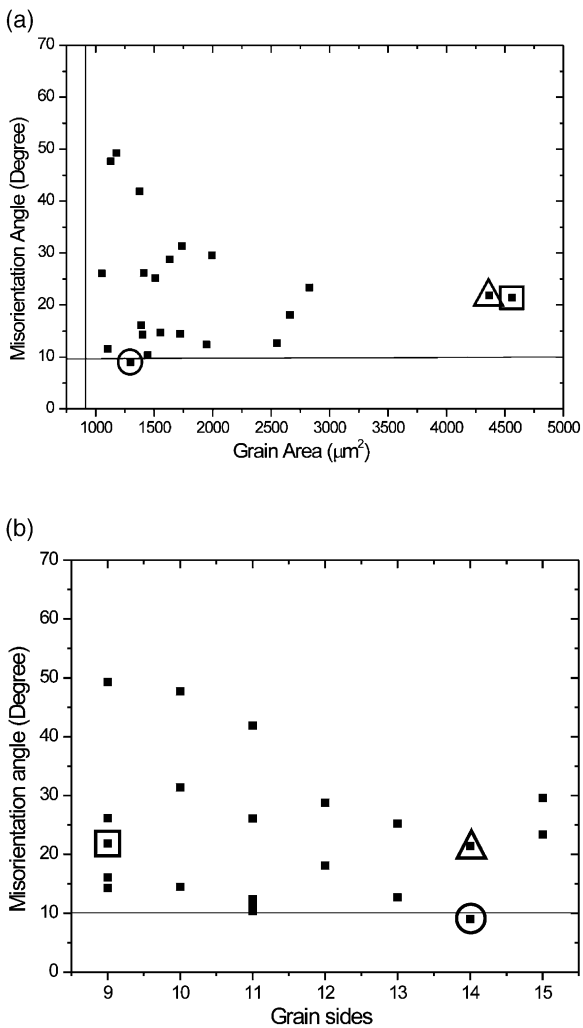

Fig. 6. Correlation between grain topology and angular deviation to the Goss orientation for large grains (measurements conducted on different areas of two samples). The same three grains are marked in both graphs. (a) Correlation between grain area (in μm^2) and angular deviation to Goss (in °). (b) Correlation between number of next neighbors and angular deviation to Goss (in °).

reveals that the large grains are not necessarily those with many neighbors and vice versa. One quite small grain (1296 μm^2 (Fig. 5b)), marked by a circle in the graph, actually has a very large number of neighbors (14) and therefore probably a high tendency to grow. Since it is also the only grain with an angular deviation to Goss of smaller than 10° this grain actually might be a Goss nucleus.

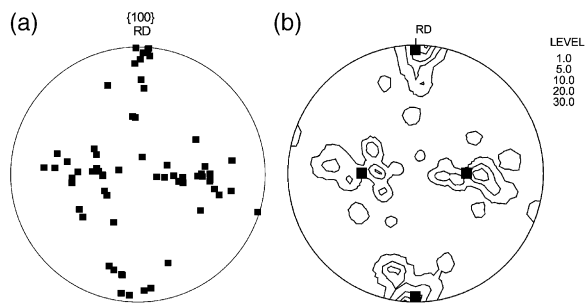

Fig. 7. (a) Discrete {100} pole figure of all large grains. (b) Continuous {100} pole figure of all large grains, weighted by grain size.

The orientation distribution of all investigated 22 large grains is shown in Fig. 7 in the form of (100) pole figures and in Fig. 8 in the form of an orientation distribution function. The left hand side of Fig. 7 shows the {100} projection points of the orientations of the large grains without considering the actual size of each grain while the right hand side pole figures are weighted by the grain size. Figs. 7 and 8 substantiate that most large grains have an orientation close to the η-fiber. However, the distribution of the intensity along the η-fiber is not homogeneous. According to Fig. 8, a maximum orientation density occurs at φ_1=0°, ϕ=33°, φ_2=0° and at φ_1=0°, ϕ=57°, φ_2=0° (symmetrically equivalent to the first). The intensity of the exact Goss orientation at φ_1=0°, ϕ=45°,φ_2=0° is relatively low. The actual maxima on the η-fiber are rotated 12–13° around the rolling direction of the sheet from the Goss orientation. In contrast to the texture of *all* grains given in Fig. 1 practically no γ- or α-fiber crystals are found among the large grains.

4. Discussion

The ODF obtained by X-ray diffraction in the s = 0.8 layer shown in Fig. 1 is a typical sub-surface texture of a primary recrystallized silicon steel. It is characterized by a weak γ-, η-, and α-fiber. While the occurrence of a pronounced γ-fiber and of a minor α-fiber is well known from textures of primary recrystallized body-centered cubic metals, the η-fiber is usually less pronounced in such

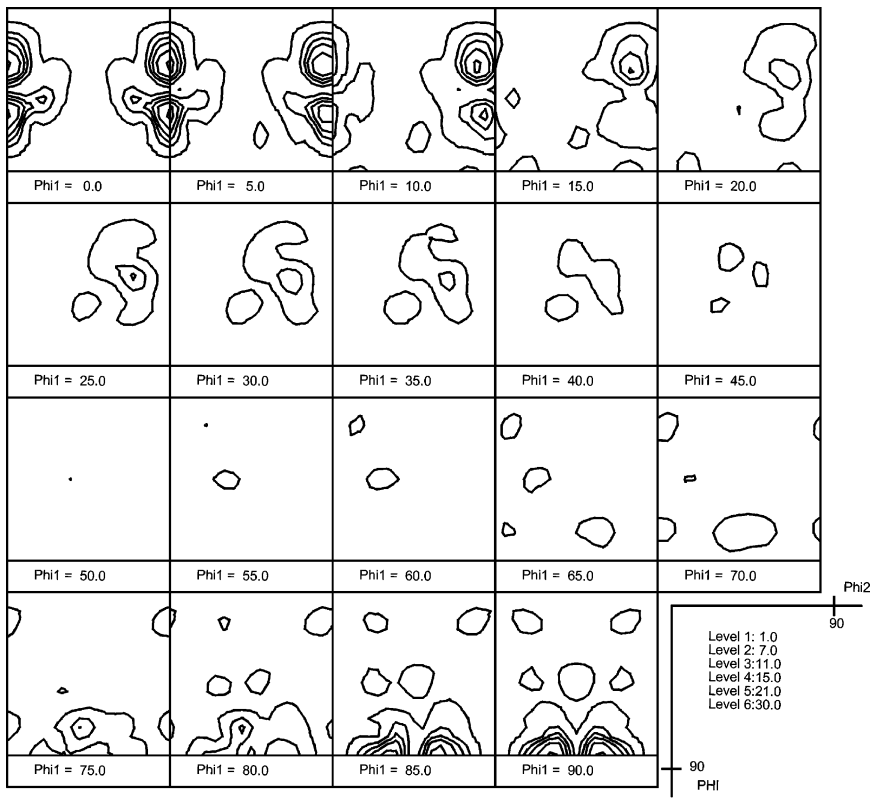

Fig. 8. ODF of large grains calculated from orientation and size of large grains.

material [14,20–24]. The η-fiber is usually found in body-centered metals if the sheet has undergone substantial friction and sub-surface shear during hot rolling. Typically, it appears stronger in steels which are alloyed with elements enlarging the high-temperature stability of the ferrite phase [25]. Depending on the further strain and annealing path, the η-fiber becomes more or less pronounced. Mishra et al. [26] reported for a high-permeability grain-oriented Si steel (using only one stage of cold reduction) a strong η-fiber with a maximum close to $\{013\}<100>$ $(\varphi_1, \phi, \varphi_2)=(0°, 18.4°, 0°)$ in the s = 0.8 layer. Fig. 1 shows that the exact Goss component at $(\varphi_1, \phi, \varphi_2)=(0°, 45°, 0°)$ is rather weak in the primary recrystallized sample. This observation is in agreement with previous work [26].

In case that topology, i.e. number of next neighbors respectively grain size plays the dominant role during secondary recrystallization and assuming further that mobility as well as energy aspects are homogeneous throughout the microstructure, the grain with the largest number of neighbors (which might be one of the largest grains) in the inspected subsurface layer of the primary recrystallized steel should be close to the Goss orientation. The ODF of the secondary recrystallized material shows a maximum deviation from the Goss orientation of about 10° and this should be the same for the grains serving as nuclei.

From the data presented in Fig. 4 no tendency is visible that grains are the closer to the Goss orientation the larger they are or the more neighbors they have. Quite the contrary, Fig. 4 shows that large grains, respectively grains with many neighbors show a similar distance to the Goss orientation as the smaller grains or grains with few neighbors.

For the 22 very large grains (Fig. 6) which all have orientations close to the η-fiber the maximum

of the orientation distribution function shows 12° deviation from the precise Goss component. It is therefore impossible to obtain a sharp Goss texture from these grains. However, one suitable Goss grain nucleus displayed in Fig. 5b and marked with a circle in Fig. 6 has been detected. Indeed, this grain is not under the very largest grains but it is a grain with a high number of neighbors, meaning that this grain is situated in an area of the primary recrystallized material with relatively small average grain size. In contrast, the two largest grains, marked by a triangle and a square in Fig. 6 have angular deviations to the Goss orientation of 21.9° and 21.4° and therefore, obviously, cannot act as typical nuclei for the sharp secondary recrystallization Goss texture. Also, one of these grains has a much smaller number of next neighbors (9) and should therefore have a comparatively low tendency to grow. The other, however, has the same number of neighbors as the possible Goss nucleus and it is not clear why this grain should, in comparison to the possible Goss nucleus, not be able to grow. It must be mentioned that the growth behavior of these areas has not been investigated yet due to experimental difficulties. It is therefore up to now not possible to make a clear statement on the importance of grain topology for the development of the Goss texture.

A comparison of Figs. 4 and 6 reveals that for a *statistical* evaluation of the topology effect on grain growth the grain size may be a reasonable measure because in a homogeneous microstructure grain area and number of next neighbors (i.e. the grains circumference) are approximately related by a square function. For a detailed discussion of *particular* grains, however, this statistically expected relationship between grain size and number of next neighbors does not need to be correct and it is very important to determine both values in order to detect possible Goss grain nuclei.

5. Conclusions

It was investigated whether a topological advantage (either size or number of next neighbors) of Goss oriented grains in the primary recrystallized microstructure could be responsible for the sharp Goss texture developing during secondary recrystallization in silicon transformer steel. Two types of measurements were carried out by automatic crystal orientation measurements (ACOM) in a field emission gun scanning electron microscope (FEGSEM) on a subsurface layer of a primary recrystallized sample. First the size, number of next neighbors and orientation distribution of a large amount of grains was determined. No tendency for large grains or grains with many next neighbors to be close to Goss grains was found. Second, the orientation distribution of particularly large grains was investigated. The large grains were mainly located on the η-fiber in Euler orientation space but the Goss orientation was only weakly occupied. The grains which were closest to the Goss orientation were not particularly large while the largest grains were more than 20° away from the Goss orientation. However, one grain which was close to the Goss orientation, although not very large, showed a particularly high number of next neighbors and might therefore be a possible Goss nucleus. Though, also some grains with a high deviation from the Goss orientation showed the same or even higher number of next neighbors and it is not clear why these grains should not also be able to act as a nuclei for secondary recrystallization. It can be concluded that an inherited topology effect alone cannot explain the dominance of the Goss texture during secondary recrystallization of silicon steel. Alternatively it might be that no relevant Goss nucleus has been observed yet. This assumption is supported by the extreme rareness of these grains because only one grain out of 10^6 in the primary recrystallized structure will grow during secondary recrystallization.

References

[1] Goss NP. Trans Am Soc Metals. 1935;23:511.
[2] Ruder WE. Asm 1935;23:534.
[3] Burwell JT. Trans. AIME 1940;140:353.
[4] Hillert M. Acta Metall 1965;13:227.
[5] Srolovity DJ, Grest GS, Anderson MP. Acta Metall 1985;33:2233.
[6] May JE, Turnbull D. Trans. AIME 1958;769:781.
[7] Shimizu R, Harase J. Acta Metall 1989;37:1241.
[8] Lin P, Palumbo G, Harase J, Aust KT. Acta Mater 1996;44:4677.

[9] Hayakawa Y, Szpunar JA. Acta Mater 1997;45:1285.
[10] Rajmohan N, Szpunar JA, Hayakawa Y. Acta Mater 1999;47:2999.
[11] Morawiec A. Scripta Metall 2000;43:275.
[12] Chen N, Zaefferer S, Lahn L, Günther K, Raabe D. In: Lee S, editor. Proceedings of the 13th International conference on Textures of Materials (ICOTOM 13). Seoul, South Korea, 2002:949.
[13] Matsuo MI. ISIJ International 1989;29:809.
[14] Inokuti, Maeda C, Itoh Y, Shimanaka H. ICOTOM6. Tokyo, 1981:948.
[15] Von Neumann J. Metal interfaces. Cleveland: American Society for Metals, 1952:108.
[16] Mullins WW. Journal of Applied Physics 1956;27:900.
[17] Smith CS. Metal Interfaces. Cleveland: ASM, 1952:65
[18] Feltham P. Acta Metall 1957;5:97.
[19] Louat NP. Acta Metall 1974;22:721.
[20] Därmann C, Mishra S, Lücke K. Acta Metall 1984;32:2185.
[21] Schlippenbach UV, Emren F, Lücke K. Acta Metall 1986;34:1289.
[22] Hutchinson WB. Int. Mat. Rev 1984;29:25.
[23] Ushioda K, Hutchinson WB, Agren J, Schlippenbach UV. Mat. Sci. and Techn 1986;2:807.
[24] Hölscher M, Raabe D, Lücke K. Steel Research 1991;62:567.
[25] Raabe DL, Lücke K. Scripta Metall 1992;26:1221.
[26] Mishra S, Därmann C, Lücke K. Metal Trans 1986;17A:1301.